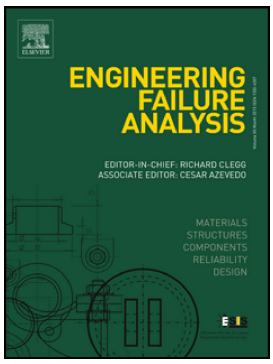

Pipe networks transporting hydrogen pure or blended with natural gas, design and maintenance

G. Pluvinage, J. Capelle, M. Hadj Meliani

PII: S1350-6307(19)30507-2

DOI: https://doi.org/10.1016/j.engfailanal.2019.104164

Reference: EFA 104164

To appear in: *Engineering Failure Analysis*

Received date: 11 April 2019

Revised date: 6 August 2019

Accepted date: 28 August 2019

Please cite this article as: G. Pluvinage, J. Capelle and M.H. Meliani, Pipe networks transporting hydrogen pure or blended with natural gas, design and maintenance, *Engineering Failure Analysis*(2018), https://doi.org/10.1016/j.engfailanal.2019.104164

PIPE NETWORKS TRANSPORTING HYDROGEN PURE OR BLENDED-WITH NATURAL GAS, DESIGN AND MAINTENANCE

G. Pluvinage[1], J. Capelle [2], M. Hadj Meliani[3],

[1] FM.C Silly sur Nied, Metz, France,
[2] LEM3, Université de Lorraine, Metz, France
[3] LPTPM, Hassiba Benbouali University of Chlef, Algeria

Abstract

Steel is subject-to hydrogen embrittlement (HE). This problem is relatively accurate for pipes transporting hydrogen pure or blended–with natural gas. Therefore this problem has to be taken into account for the design and maintenance of pipe networks for this kind of transport. Design needs to modify the design factor for computing maximum working pressure in this case. Defect harmfulness needs specific tools for each type of defect which are the same-as for pipe transporting natural gas, but the admissibility criterion is modified when transporting hydrogen.

For cracking, harmfulness is determined with a failure assessment diagram with steel fracture toughness under HE. For defect correction, the estimated repair factor (ERF) is changing due to modification of the flow stress. For gouging, the Constraint Modified Failure Assessment Diagram (CMFAD) incorporates the actual material failure master curve. For dents, the criterion proposed by Oyane et al take into account the major reduction of elongation at failure. The influence of HE on fatigue endurance is seen through the fatigue assessment diagram(fAD). Discussion is based on recategorisation of defect, assessment tools, embrittlement and fatigue life duration.

Key words : Hydrogen Embrittlement, Pipe Steels, Defect Assessment

1.INTRODUCTION

Apart from pipelines operating under pressure with pure hydrogen, this gas can be introduced into oil and gas installations by contamination during manufacturing processes, treatments such as carbonization, cleaning, pickling, phosphating, electrochemical cleaning, electro-plating, profiling, machining and drilling (lubricating effect), welding or brazing during manufacturing. It may be present in structural elements under cathodic protection such as pipes and tanks for storing and transporting crude oil. Different reactions occur during corrosion: in the anodic part, there is dissolution of the material (reduction of oxygen) with production of hydrogen in the cathodic part.

Hydrogen is is considered as energy carrier for fuel cell electric vehicles (FCEVs). Blending hydrogen into the existing natural gas pipeline network has been proposed as a means of

increasing renewable energy systems. Its implementation is generally considered with relatively low concentrations, less than 5%–15% hydrogen by volume, but high concentration up to 50% are also investigated. Durability and integrity of the existing natural gas pipeline network is an open question because hydrogen greatly degrades mechanical properties of steel as we can see in figure1. This phenomenon is called hydrogen embrittlement (HE). Tensile tests perform on API L X52 pipe steel with specimens loaded in air and after hydrogen introduction by an electrolytic process under a potential of V = -1 Volt. It can be seen on figure 1 that elongation at failure is greatly reduced (38%) and yield stress (3.8%) and ultimate strength (7.4%) are less affected. This hydrogen embrittlement of steel was first discovered by Johnson [1].

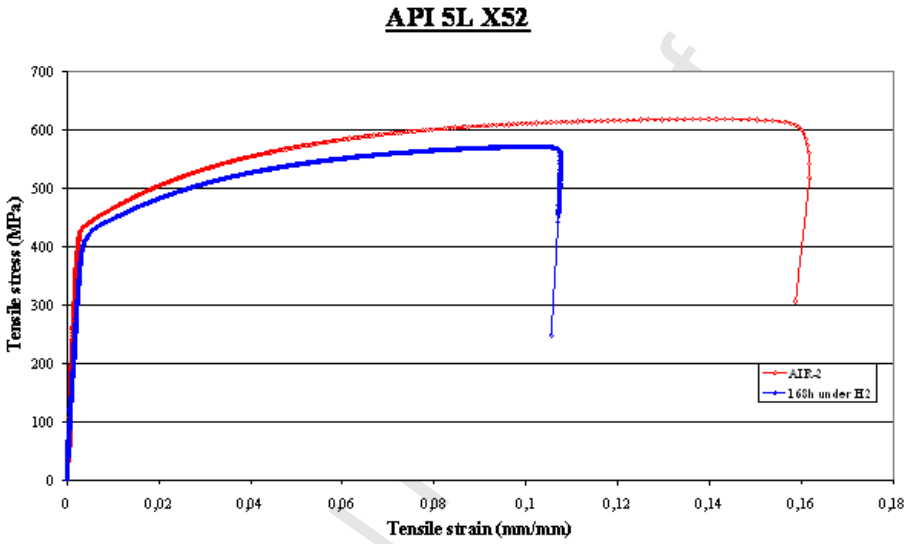

Fig.1 : Tensile test on API L X52 pipe steel with specimens loaded in air and after hydrogen introduction by electrolytic process under a potential of V = -1 Volt

This embrittlement is associated with a reduction of fracture resistance. Capelle et al [2] noticed that the work done for fracture initiation U_i decreases suddenly for hydrogen concentration higher than a critical one C_H^* where the material becomes brittle as can be seen on the fracture area in figure 2. These authors determined that the critical hydrogen concentration is a power decreasing function of yield stress σ_y and ultimate strength σ_{ul}, equation 1.

$$C_H^* = B_1 \sigma_y^{n_1}$$
$$C_H^* = B_2 \sigma_{ul}^{n_2} \quad (1)$$

where B_1, B_2, n_1 and n_2 are material constants.

Hydrogen induced cracking is a type of damage often referred to as HIC (Hydrogen induced cracking). This cracking occurs when high amounts of hydrogen are introduced into the material, of the order of several ppm. Hydrogen supersaturation can recombine in the form of molecular hydrogen on matrix interfaces, causing microstructure defects (inclusions, carbide, etc.). This generates a considerable internal pressure that allows initiation and propagation of a crack. This type of damage is observed in pipes made of low and medium strength steel.

Stress-oriented hydrogen embrittlement cracking (SOHIC) occurs most often in thick tubes and results from hydrogen enrichment of segregated zones. The solubility of hydrogen is lower in the ferritic zone which leads to a cracking of the matrix by diffusion of hydrogen, figure. 3.

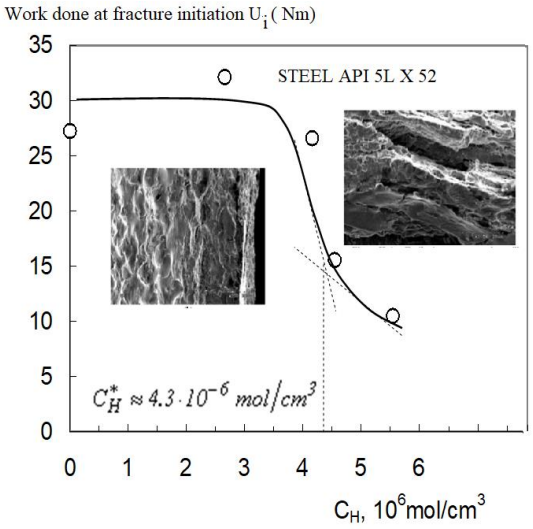

Fig.2 : Influence of hydrogen concentration on work done at fracture initiation and fracture surface aspect; API 5L X52 pipe steel.

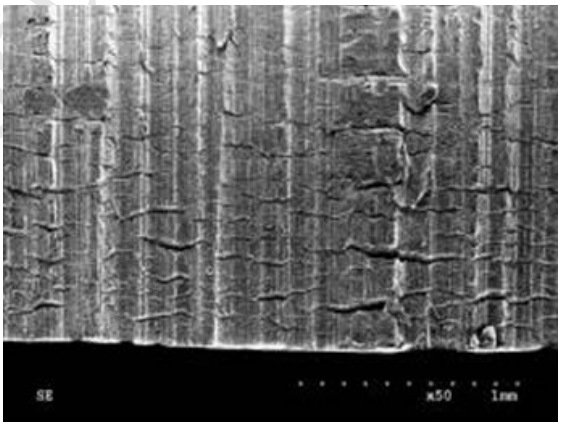

Fig.3 : Stress-oriented hydrogen embrittlement cracking (SOHIC) in pipe steel API 5L X52.

SOHIC zones are considered as a loss of metal in code API 579-1 [3]. The remaining strength factor (RSF) is similar to the relative effective thickness according to equation 2

$$RSF = \frac{1 - \frac{(w_H - FCA).D_H}{t_c}}{1 - \frac{1}{M_t}\frac{(w_H - FCA).D_H}{t_c}} \quad (2)$$

- w_H thickness of SOHIC
- D_H damage parameter D_H =0.8
- M_t Folias factor

$$M_t = \sqrt{1 + 0.4025\lambda^2} \quad (3)$$

$$\lambda = \frac{1.285s}{\sqrt{Dt_c}} \quad (4)$$

After dissociation of molecular hydrogen into atoms, hydrogen is transported into metals by diffusion or by dislocation. The general process of hydrogen embrittlement is presented in figure 4 according to a scheme proposed by Thompson [4].

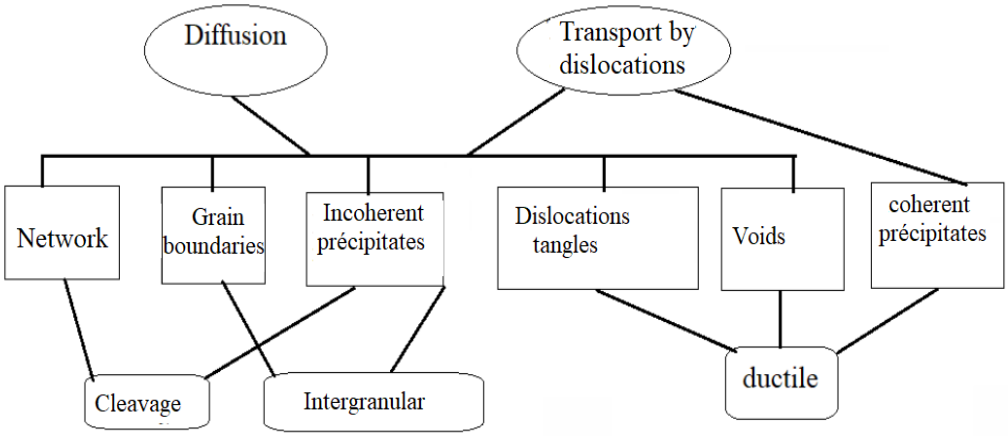

Fig.4 : scheme of the general process of hydrogen embrittlement [4].

Several mechanisms are invoked, namely:
• weakening of metal-metal atomic bonds
• modification of plasticity,
• decohesion / dislocation competition
• molecular recombination on defects,
• stress triaxiality

The aim of this paper is to see how hydrogen embrittlement, modify pipe defect assessment. This problem is not simple because there are a large variety of defects (crack, gouge, dente

corrosion defect and combined defect). Therefore pipe defect harmfulness is examined trough different tools as Failure Assessment Diagram (FAD), Estimated Repair Factor (ERF), Notch Failure Assessment Diagram (NFAD), Domaine Failure Assessment Diagram (DFAD) and estimated through Safety Factor (FS). These assessment tools are based on materials properties such as fracture toughness, yield stress, ultimate strength and elongation at failure which are more and less sensitive to HE. Therefore, for pipe transporting hydrogen pure or blended; it is necessary to know if the safety factor remains acceptable for any detected defect. Some examples of reduction of safety factor and for different types of defect (crack, gouge corrosion defect) are presented. The acceptable safety factor needs to be guaranty during life duration of a pipe in presence of initial acceptable defect when transporting hydrogen. This can be done using Fatigue Assessment Diagram (fAD).

Trends are to use failure probability instead deterministic safety factor. Here we show that this approach needs to use specific design factor for hydrogen transportation.

2. THE INFLUENCE OF HYDROGEN EMBRITTLEMENT ON PIPE CRACK HARMFULLNESS

Very long pipes are made by welding in situ. In the weld or in the heat affected zone (HAZ). porosities, slag inclusions, melts or cracks can be detected. Cracks are considered as the most severe defects and usually have an irregular shape. They are considered as flat elliptical for internal cracks and semi-elliptical for surface cracks by a procedure of enclosing the irregular defect in a rectangle of length 2c and width 2a for internal cracks and length 2c and depth a for surface cracks. This procedure is conservative The applied stress intensity factor of a semi-elliptic crack k_{ap} is calculated according to the Newmann-Raju solution [5] valid for surface or internal defects.

2.1 Failure Assessment diagram

The Failure Assessment Diagram (DFAD) methodology is a two-parameter fracture criterion in order to have a plane representation where non-dimensional crack driving force and non-dimensional applied stress are the coordinates. The applied non-dimensional crack driving force is defined as the ratio of applied stress intensity factor K_{ap} to the fracture toughness of the material K_{Ic}.

$$k_r^* = {K_{ap}}/{K_{Ic}} \tag{5}$$

The *J* integral or crack opening displacement define also the applied non-dimensional crack driving force as:

$$k_r^* = \sqrt{{J_{ap}}/{J_{mat}}} \; or \; k_r = \sqrt{{\delta_{ap}}/{\delta_{mat}}} \tag{6}$$

where J_{ap}, δ_{ap} are the applied *J* integral and crack opening displacement and J_{mat} or δ_{mat} are fracture toughness in terms of the critical values of *J* Integral or crack opening displacement

of the material. Non-dimensional stress is described as the ratio of the gross stress over flow stress ($L_r = \sigma_g/\sigma_0$) chosen as yield stress σ_Y, ultimate stress σ_{ul} or classic flow stress $\sigma_0 = (\sigma_y + \sigma_{ul})/2$

Any kind of rupture (brittle, elastoplastic or plastic collapse) can be represented by an assessment point in FAD with coordinates L_r^*, k_r^* . Critical values of $k_{r,c}$ and $L_{r,c}$ define a critical curve (or failure curve).

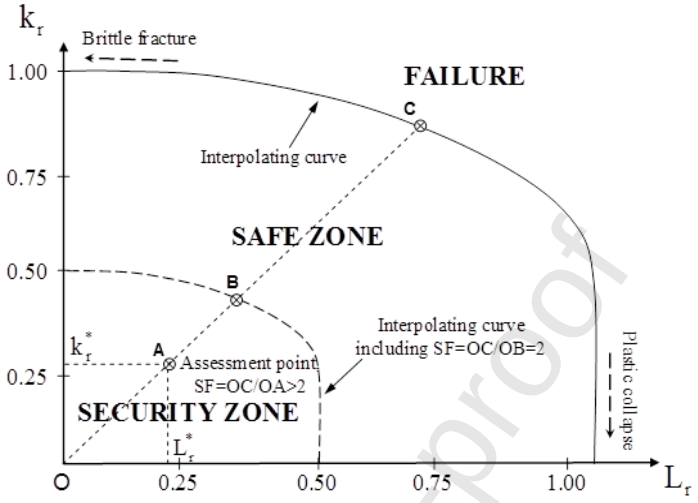

Fig. 5: Typical presentation of Failure Assessment Diagram (FAD).

The failure curve $k_{r,c} = f(L_{r,c})$ delineates a fracture design curve according to the available codes, e.g. SINTAP [6], R6 [7] and RCC-MR [8].

As a consequence of L_r and k_r definition, the loading path OC is linear when the load increases from 0 to the critical load P_c. Under service conditions, a defect in a given material is represented by an assessment point B of coordinates L_r*and k_r*. If this assessment point is inside the safe zone, no failure occurs, while if the assessment point is on the assessment curves or above, critical conditions are reached. The deterministic safety factor associated with the defect situation is simply defined by the relationship:

$$f_s = OC/OB \tag{7}$$

The criticality of the situation is generally given by comparing the obtained safety factor to the conventional value of f_s= 2.

2.2 Influence of the pipe steel on the defect assessment point

10 pipe steels have been chosen because simultaneously yield stress σ_y, ultimate strength σ_{ul} and fracture toughness K_{Ic} under hydrogen gas pressure (6.9 MPa H2) are known. API 5 L 80 steel is also considered, however a fracture test was made under high hydrogen pressure of 300 bar (30.5 MPa) [8]. The mechanical properties of these steels after hydrogen embrittlement are given in Table 1.

The assessment points associated with these steels and with the same defect are shown in figure 6. It should be noted that the position of the assessment points is further and further from the failure curve as the yield stress of the steels increases. Metallurgical progress over time will be noted: newer steels have a higher yield stress while simultaneously increasing

their toughness, which is only possible by acting on the microstructure and inclusion cleanliness.

API 5L X 80 steel has an operating point outside this general trend. The toughness of this steel obtained only by [8] is very low for reasons that can be linked in part to the very high pressure of hydrogen gas of 300 bars. The fracture J_c was measured on notched CT specimens (width W = 40 mm, thickness B = 10 mm, net thickness B_n = 8 mm) tested with and without HE.

Table 1: Mechanical characteristics of pipe steels after hydrogen embrittlement under gas pressure.

Steel	σ_y (MPa)	σ_{ul} (MPa)	σ_0 (MPa)	K_c (MPa√m)	K_{IH}/K_c %
1080	414	784	599	111	71
A 516	364	551	457,5	102	68
API 5L Grade B	299	518	408,5	89	74
API5L X 42	331	490	410,5	69	46
API5L X 46	374		187		NC
API5L X 52	429	597	513	108	50-97
API 5L X 60	422	590	506	142	73
API 5L X 65	506	611	558,5	180	49.5
API 5L X 70	566	653	609,5	197	48-95
API 5L X 80	566	707	636,5	56	6

The non-dimensional crack driving force incorporates as denominator the fracture toughness of the material. For pipe steels, it decreases after HE. However for a large scatter and yield stress range [350-600 MPa], fracture toughness decreases by 33% as mean values. Fracture toughness reduction increases with an increase of hydrogen pressure and by decreases of potential for HE ~~by~~ electrolytically –. In figure 8, the ratio of fracture toughness of 10 pipe steels listed in table 1 after ~~HE~~ and without HE is entered. Results concern tests under gas pressure of 6.9 MPa and electrolytic potential of -1 volt. In this case, the value of the K_{IH}/K_{IC} ratio is greater for the electrolytic method (K_{IH} fracture toughness after HE and K_{IC} fracture toughness in standard conditions).

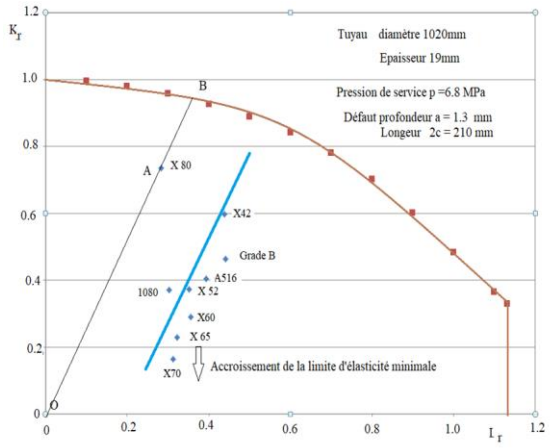

Fig.7: Assessment points of a semi-elliptical surface crack (depth 1.3mm, length 210 mm) for 10 pipe steels submitted to hydrogen embrittlement.

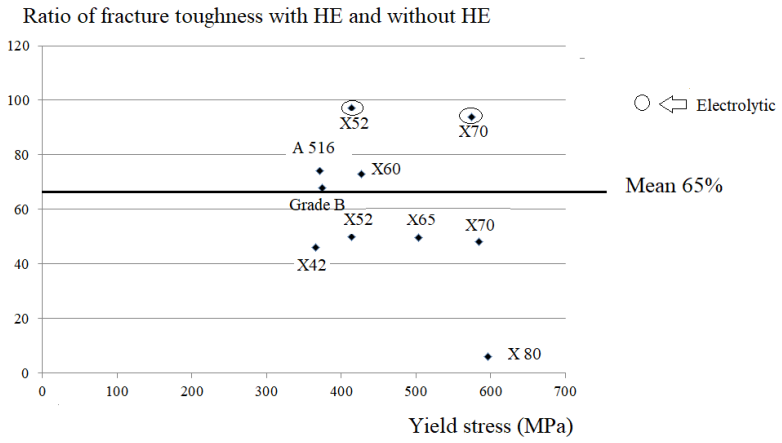

Fig.8: The ratio of fracture toughness under HE and in standard condition for 10 pipe steels.

2.2 Influence of hydrogen on the loading path in FAD

From definition of FAD parameters k_r and L_r, it results that they are both proportional to gross stress. Therefore the loading path $k_r = f(l_r)$ is linear. Due to the reduction of fracture toughness by hydrogen embrittlement HE, the non-dimensional crack driving force k_r decreases with HE. The loading parameter is little affected by HE because it has practically no effect on flow stress.

Here we consider a pipe subjected to internal pressure made from API 5L X52 steel. The pipe has a diameter D = 611 mm and thickness t=11 mm. This pipe exhibits an internal semi-elliptical crack at the pipeline with a defect depth over thickness ratio a/t = 0.5 and aspect ratio a/c = 0.5. Figure 9 shows that the loading path under HE is above the loading path for conditions without HE. This induces consequence on modification of the safety factor.

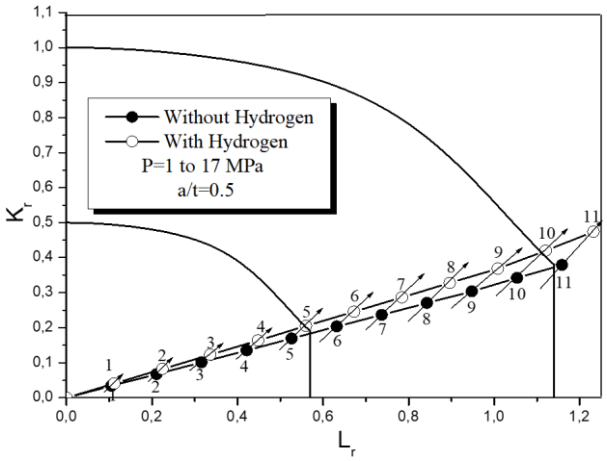

Fig.9: Modification of loading path under HE; pipe submitted to internal pressure made from API 5L X52 steel. Pipe diameter D=611 mm and thickness t=11 mm, relative defect depth a/t/0.5.

2.3 Influence of hydrogen on the safety factor in FAD

Safety factors have been computed according to equation 7 for the same pipe submitted to 2 values of internal pressure (p = 5 and p = 11 MPa). Semi-elliptical defect sizes have 5 different ~~5~~ values (a/t = 0.1, 0.2, 0.3, 0.4 and 0.5) and the aspect ratio is a/c = 0.5. One notes that the safety factor decreases when the defect becomes deeper. Failure occurs only for high pressure (p =11 MPa) and for deep defects (a/t = 05 without HE and a/t = 0.4 and = 0.5 with HE see table 2).

Table 2**:** Safety factor (f_s) values for different relative crack depth ratios (a/t=0.1 to 0.5), with and without HE and for 2 different gas pressures (p =5 MPa and 11 MPa).

a/t	p = 5 MPa			P =11 MPa		
	f_s		Diff. (%)	f_s		Diff. (%)
	Without H_2	With H_2		Without H_2	With H_2	
0.1	3.85	3.70	3.85	1.79	1.64	8.93
0.2	3.45	3.12	10.34	1.56	1.41	10.93
0.3	3.03	2.63	15.15	1.37	1.20	13.70
0.4	2.63	2.22	18.42	1.18	Failure	
0.5	2.17	1.89	15.21	Failure	Failure	

3) CORROSION DEFECT HARMFULLNESS AFTER HE

Corrosion defects are characterized by 3 dimensions: depth (a), length (2c) and width (W). The failure of a corrosion defect considered as semi-elliptical, is controlled by its size and the flow stress σ_0 of the material. The input parameters include pipe outer diameter (D), wall thickness (t), specified minimum yield strength (σ_y), maximum allowable operating pressure (MAOP), longitudinal extent of corrosion (2c) and defect depth (d). Numerous solutions of limit pressure for corrosion defects are proposed in codes and literature limit load analysis

(ASME B31G [10], modified ASME B31G [11], DNV RP-F101 [12] and Choi et al. [13]). The limit pressure p_L (which is less than the burst pressure p_c) is generally expressed as:

$$p_{L=\frac{2t}{D}.\sigma_0}.\left[\frac{1-\alpha\left(\frac{a}{t}\right)}{1-\alpha\left(\frac{a}{t}\right).\frac{1}{M}}\right] \quad (8)$$

M is the Folias correction taking into account the pipe curvature σ_0 flow stress, α a geometrical parameter and Folias correction are different according to the applied method. Flow stress is generally a simple function of yield stress or ultimate strength

As we can see on figure 9, these two mechanical parameters are little affected by HE. In this figure the ratio of these two parameters with and without HE is entered for 5 pipe steels (API 5L X42, X52, X65, X80 and X100). This ratio is generally less than 10%. Therefore the calculated limit pressure is little affected by hydrogen.

The most commonly used defect assessment method is ASME B31G for the purpose of calculating the safe operating pressure associated with each corrosion defect. The safe operating pressure is the working pressure. The ratio of MAOP and the safe operating pressure P_{safe} is the estimated repair factor ERF. Necessity for repair is given by the following criterion:

$$\mathrm{ERF} = \frac{\mathrm{MAOP}}{\mathrm{p_{safe}}} \leq 1 \text{ or } 0.95 \quad (9)$$

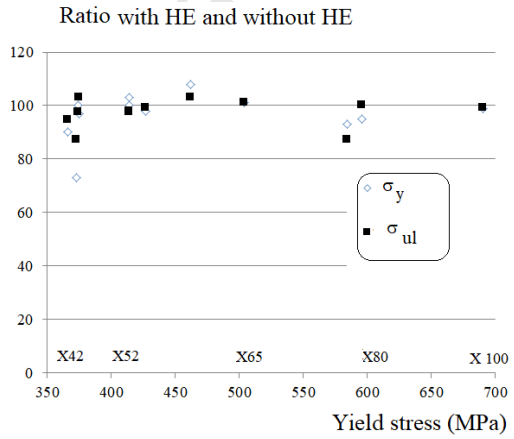

Fig. 8: Evolution of the ratio of yield stress and ultimate strength with and without HE for 5 pipe steels (API 5L X42, X52, X65, X80 and X100).

An ERF greater than one requires repair or lowering of the MAOP. The defect assessment point (2c*; a*/t) is entered in a graph of the defect length and relative defect depth coordinates (2c ; a/t). On the same graph, the curve corresponding to condition ~~is~~ ERF = 1 is also entered. A defect with an assessment point below this defect assessment curve is acceptable. Any defect with an assessment point above requires repair or working pressure de-rating. One

notes that the defect assessment curve depends on the method (B31 or B31 mod) to compute p_{safe} or p_L. It depends also on MAOP, pipe thickness and diameter and material flow stress σ_0. An example of an assessment diagram is given in figure 9.

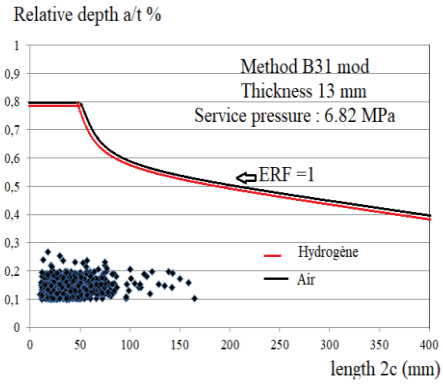

Fig.9: Estimated repair factor ERF plotted in a relative graph of defect depth vs defect length.

4) GOUGE HARMFULLNESS AFTER HE

A gouge in a pipe can be likened to a notch, figure 10. The latter is characterized by three geometric parameters: its depth a, its angle Ψ and its radius ρ. A crack can be considered as a particular case of notch with Ψ= ρ =0.

Fig 10: Example of gouges on a pipe surface provoked by a scrapers.

4.1 The notch fracture toughness

Failure emanating from a notch is treated by Notch Fracture Mechanics [14] based mainly on a local criterion. Among these criteria, Volumetric Method [14] is a local stress criterion which supposes that the fracture process rupture requires a certain volume. This volume is supposed to be a cylindrical one whose diameter corresponds to the effective distance. The physical significance of this fracture process volume is the "highly stressed region" where the required energy release rate is stored. The difficulty is to find the limit of this zone. This limit is not a material constant, but depends on the loading mode, geometry of the structure and the load level. The effective distance X_{ef}, which represents the diameter of this supposedly

circular zone according to the previous assumption, is obtained by examining the distribution of the opening stresses.

The elastic-plastic stress distribution along the ligament is presented in a bi-logarithmic diagram (figure 11). It has three distinct areas. The elastic-plastic stress increases mainly and reaches a peak value (zone I) and then gradually decreases to the elastic state (zone II). Zone III represents the linear behavior in the bi-logarithmic diagram. It has been proved by examination of fracture initiation sites that the effective distance corresponds to the beginning of zone III which is in fact a point of inflection of this stress distribution. A graphical method based on the relative stress gradient associates the effective distance with the minimum of χ, the relative stress gradient. χ is given by equation 10 where σ_{yy} is the maximum principal stress or opening stress.

$$\chi(r) = \frac{1}{\sigma_{yy(r)}} . \frac{\partial \sigma_{yy(r)}}{\partial r} \tag{10}$$

The effective stress σ_{ef} is then considered as the average value of the distribution of stresses over the effective distance. However, stresses are multiplied by a weighting function in order to take into account the stress gradient due to the geometry and the loading mode and the action distance r. The distribution of stress is then given by:

$$\sigma_{ef} = \frac{1}{X_{ef}} . \int_0^{X_{ef}} \sigma_{yy}(r) . \Phi(r) . dr \tag{11}$$

A description of the stress distribution at a gouge tip and the procedure using the relative stress gradient to find the effective distance is given in figure 11.

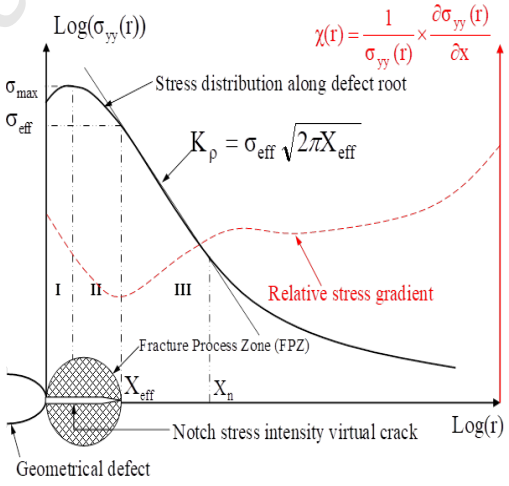

Fig. 11: Schematic distribution of elastic-plastic stresses along a ligament ahead of a gouge. Determination of effective distance.

The Notch Stress Intensity Factor (NSIF) K_ρ is defined as a function of the effective distance and stress σ_{ef} and X_{ef} by:

$$K_\rho = \sigma_{ef}\left(2\pi X_{ef}\right)^{\alpha} \tag{12}$$

α is the slope of the stress distribution in region III. The fracture criterion is expressed by:

$$K_\rho = K_{\rho,c} \tag{13}$$

$K_{\rho,c}$ is the notch fracture toughness of the material. It was found that the notch fracture toughness increases linearly with the square root of the notch radius when it is greater than a critical value ρ_c [15]. For steel, ρ_c is of the order of a few tenths of a millimeter. Below this critical radius, $K_{\rho,c}$ is constant and equal to K_{Ic}, the conventional fracture toughness measured with a cracked specimen ($\rho = 0$).

$$K_{\rho,c} = K_{I,c} \text{ pour } \rho \leq \rho_c$$

$$K_{\rho,c} = K_{I,c} + A.\sqrt{\rho} \text{ for } \rho > \rho_c \tag{13}$$

The additional contribution $A.\sqrt{\rho}$ corresponds to the plastic work when the notch plastic zone invades the ligament. The size of the plastic notch area is equal to that of the ligament when the notch radius reaches its critical value.

4.2 Effect of constraint on notch fracture toughness

Constraint is defined as the resistance of a structure against crack-tip plastic deformation. Two methods are used to define the constraint:

i) Analysis of modification of crack tip distribution by geometrical or loading parameters,

ii) Analysis of the plastic zone size after the same kind of modifications.

If we compare the stress distribution obtained in a reference stress situation (generally small-scale yielding) to another general one, it is modified in two ways: there is a shift and a small rotation. These modifications of the stress distribution are used as transferability parameters. The shift of the stress distribution is used to define several plastic constraints.

For a crack, Larson et al. [16] suggested describing the elastic stress field at the crack tip by three terms, and introduce for the first time the term T as the second in a series as a constraint parameter:

$$\sigma_{ij} = \frac{K_{ij}}{\sqrt{2\pi r}} f_{ij}(\theta) + T\delta_{1i}\delta_{1j} + O\sqrt{r} \tag{14}$$

Therefore, ideally T stress is a constant stress that acts along the crack direction and shifts the opening stress distribution according to the sign of this stress. For some particular θ angles,

the T stress is given by particular values of the difference between the opening stress σ_{yy} and the stress parallel to the crack σ_{xx}. Particularly for $\theta = 0$, the T stress is given by:

$$T = \left(\sigma_{xx} - \sigma_{yy}\right)_{\theta=0} \tag{15}$$

Equation (15) is the basis of the so-called stress difference method, which was proposed by Yang et al. [17]. The stress distribution in the direction $\theta = 0$ is generally computed by the Finite Element method.

Hadj Meliani et al. [18] pointed out the effect on notch fracture toughness $K_{\rho,c}$ of critical constraint described by the critical effective T stress parameter $T_{ef.,c}$. Fracture toughness decreases linearly with the constraint according to:

$$K_{\rho,c} = \alpha\, T_{ef,c} + K^0_{\rho,c} \tag{16}$$

where $K^0_{\rho,c}$ is the reference fracture toughness corresponding to $T_{ef,c} = 0$, which is considered as close to the small-scale yielding situation. α a material constant $\alpha = -0.069$ and $K^0_{\rho,c} = 77.3\ \text{MPa}\sqrt{\text{m}}$ for the API X52 pipe steel.

Bouledroua et al [19] assume that the constraint T is proportional to loading. This assumption is true for elastic behavior, but can be extended if fracture occurs with little plasticity.

The non-dimensional loading parameter L_r is described as the ratio of the gross stress σ_g to the flow stress σ_0 or as the ratio of the applied load P to the limit load P_L:

$$L_r = \sigma_g/\sigma_0 \quad or \; L_r = P/P_L \tag{17}$$

The non-dimensional constraint is proportional to the loading parameter as:

$$\frac{T}{\sigma_y} = \beta_T L_r \tag{18}$$

β_T is a coefficient of proportionality and is obtained for different levels of loading represented by the non-dimensional loading parameter L_r assuming elastic behavior until cut for $L_{r,max} = 1.2$.

The Material Failure Master Curve (MFMC) is described by equation 16, which can be rewritten as equation 19:

$$K_{\rho,c} = K^0_{\rho,c}\left[1 + \Lambda L_{r,c}\right] \tag{19}$$

where

$$\Lambda = \frac{\alpha \beta_{T\sigma_y}}{K^0_{\rho,c}} \tag{20}$$

α is the material parameter of equation (3), σ_y yield stress and $K^0_{\rho,c}$ the reference fracture toughness with T_{ef}=0.

Table 3: values of material parameters of steel APIL 5L X52

	With HE	No HE
α	-0,074	-0,084
β_T	-0,793	-0,793
σ_y (MPa)	450	431
$K^0_{\rho,c}$ (MPa$\sqrt{m}$)	82,6	95,6
Λ	0.31	0.30

Table 3 gives the value of the different parameters of equation 20 with and without HE. One notes that yield stress, α and β_T are HE sensitive material parameters. Parameter β_T depends only on structure geometry and loading mode;

4.3 Constraint Modified Failure Assessment Diagram (CMFAD)

The ordinate of the defect assessment point is given by the non-dimensional driving force k_r^*:

$$k_r^* = {K_{ap}}/{K_{mat}} \tag{21}$$

where K_{ap} is the applied notch stress intensity factor and K_{mat} is the fracture toughness of the material, which can be the notch fracture toughness $K_{\rho,c}$ instead of classical fracture toughness K_{Ic}.

In the traditional approach, the material fracture toughness is considered as determined according to standard with a high constraint specimen. This value can be identified as $K_{mat} = K^0_{\rho,c}$. Therefore, a reference value of $k^*_{r,T=0}$ is given by:

$$k^*_{r,T=0} = {K_{app}}/{K^0_{\rho,c}} \tag{22}$$

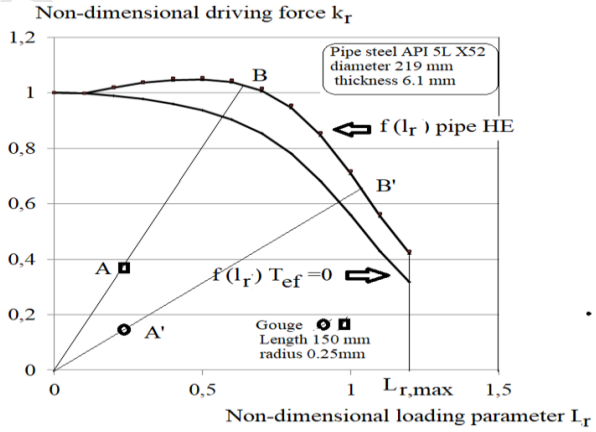

Fig. 12: Constraint modified failure assessment diagram with failure assessment curves $f(L_r)_{T=0}$ and $f(L_r)_{pipe}$ with and without HE.

In order to reduce the conservatism induced by the use of a high constraint specimen for fracture tests, and taking into account the increase of fracture toughness by the loss of constraint, we define the coordinates of the assessment point devoted to a pipe submitted to internal pressure by:

$$k^*_{r,pipe} = {K_{ap}}\Big/{K_{\rho,c(T)}} \tag{23}$$

The failure assessment curve for any value of constraint T is given as:

$$k_{r,c} = f(L_{r,c}).[1 + \Lambda L_{r,c}] \tag{24}$$

The failure assessment curve given by equation 24 is called $f(L_r)_{pipe}$. The reference failure assessment curve is called $f(L_r)_{T=0}$.

Both curves are plotted in figure 12. The failure assessment curves $f(L_r)_{struct}$ lies above the reference curve. There is practically no difference between the curve with HE and without HE because for both parameters Λ_{HE} and Λ_{noHE} are very close.

4.4 Assessment of a gouge in a pipe after HE

In the following example, a longitudinal gouge located on the surface of an API 5L X52 steel pipe is analyzed. The gouge has a length of 150 mm, an angle Ψ of 45 ° and a notch radius of 0.25 mm. The circumferential stress derived from an operating pressure of 70 bars is entered in table 4 as well as the coordinates of the assessment point L_r^* and k_ρ^*.

Dimensions of the pipe are: thickness 6.1 mm and diameter 219.1 mm. Fracture toughness and flow stress under HE for steel API 5L X 52 are taken into account in the establishment of the parameters L_r^* and k_ρ^*

The safety factors have been obtained from the assessment points coordinates from equation 7 and entered in table 4 for classical FAD and CMFAD.

Table 4: Summary of the values of L_r and $K_{\rho,r}$ for a gouge located on pipe surface

	$K_{\rho,ap}$ (MPa√m)	$K_{\rho,c}$ (MPa√m)	$\sigma_{\theta\theta}$ (MPa)	σ_y (MPa)	σ_{ult} (MPa)	σ_0 (MPa)	L_r^* and k_ρ^*
Without HE	14.6	95.6	125.7	431	526	478.5	(0.26 ; 0.15)
With HE	14.6	82.6	125.7	450	547	498.5	(0.25 ;0.35)

Tableau 5 : safety factor of a gouge with and without HE

	Safety factor		
	No HE	With HE	Influence (%)
FAD	4.40	2.84	55
CMFAD	4.18	2.5	67

The safety factor is decreased after hydrogen embrittlement of about 55%, however the notch fracture toughness has decreased by 13.5% The coefficient of safety under hydrogen, is greater than 2, the coefficient generally adopted in design.

5. DENTE HARMFULLNESS AFTER HYDROGEN EMBRITTLEMENT

A dente in a pipe introduces localized strains and causes strain hardenings in the material. The high stresses and strains caused by the dente are accommodated by the ductility of the metal. Results of full-scale burst tests have confirmed this by showing that dentes generally do not affect the resistance to bursting of the pipe and that outward movements allow the pipe to regain its original circular shape. In the literature, some acceptable depth limits are proposed. Evaluation is usually done by empirical rules. If the depth is greater than one tenth of the diameter of the pipe, repair is mandatory. It has been seen that dente depths of up to 8% of the pipe diameter [20] and possibly up to 24% [21] do not significantly reduce the burst strength of a pipe. The API code 579 [3] relates to the treatment of dents without scratches (smooth). Dentes are dangerous if they occur on longitudinal weld seams because cracks can develop. Many sources report that dented weld seams can have very low burst pressures. The European Pipeline Research Group (EPRG) [22] has proposed a criterion for acceptance of smooth recesses located away from pipe weld seams, with membrane stress levels below 72% of the yield limit:

$$\frac{h}{D_e} \leq 10\% \tag{23}$$

where depth h is the depth of dente in the unpressurized state and the outside diameter of the pipe. The internal pressure of the pipe tends to push back the dent, thus reducing its depth. The depth measured on the pipeline in service must therefore be corrected before this criterion can be applied. EPRG has proposed a correlation between the depth of dent on unpressurized pipe h_0 and pressurized one h [3]:

$$h = 1.43\, h_0 \tag{24}$$

The EPRG limit for a smooth dent in a pressure pipe is:

$$\frac{\mathrm{h_0}}{\mathrm{D_e}} \leq 7\% \tag{25}$$

Prediction on failure of a pressurized pipe with a dente is based on the idea that it results from an indentation process.

A ductile failure criterion generally used for deep drawing is proposed. The criterion proposed by Oyane et al. [38] is used:

$$I = \frac{1}{C_2}\int_0^{\overline{\varepsilon_f}} \left(C_1 + \frac{\sigma_h}{\bar{\sigma}}\right) d\bar{\varepsilon} \tag{26}$$

where ε_f is the equivalent failure strain; σ_h the hydrostatic stress; $\overline{\sigma}$ the equivalent stress; $\bar{\varepsilon}$ the equivalent deformation; and C_1 and C_2 are material constants.

To determine the constants of material C_1 and C_2, two tests must be performed in two types of stress conditions: a uniaxial stress and a plane strain test. Constant C_2 is easily obtained by a simple tensile test where C_2 is equal to elongation at failure. The constant C_1 is obtained by a burst test on a smooth pipe.

It was noted that elongation at failure is very sensitive to hydrogen embrittlement as it can be seen in figure 13. The ratio of elongation at failure with and without hydrogen embrittlement decrease linearly with yield stress and its value is about 0.5 for 900 MPa yield stress.

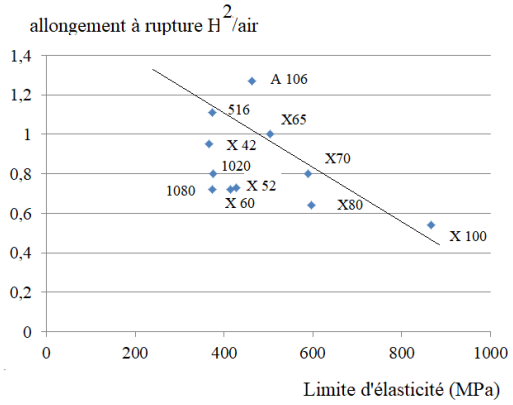

Fig 13: Ratio of elongation at failure with and without hydrogen embrittlement. Influence of yield stress.

By finite element simulation (EF), Integral I is calculated for each element and each deformation step. The mechanical properties of the studied steel are those of the API 5L X52 steel for which the failure elongation is 31.5% and after introduction of hydrogen of 23%. The results of finite element calculations of the integral I of Oyane's criterion as a function of the dente depth are presented in figure 14. It is noted that the damage is much more severe when the steel is subjected to HE.

6. INFLUENCE OF HE ON THE FATIGUE ENDURANCE OF PIPE STEEL

Fatigue endurance after hydrogen embrittlement is a subject that does not seem to have been discussed extensively in the literature. However, this is an extremely important area since the fatigue life with a large number of cycles is given as 70 to 90% initiation time. Fatigue studies after hydrogen embrittlement mainly concern long cracks propagation in the field of the Paris law regime. It should be noted that it is unlikely because of frequent non-destructive testing that non tolerated a long crack in a pressurized line.

The fatigue resistance at initiation of the API 5L X52 steel was measured in a radial direction at room temperature using non-standard curved notched specimens, namely, "Roman tile" specimens [24]. The specimen shape is a circle arc, corresponding to a central angle of 160° of 60 mm length. The V-notch with the notch opening angle of 45° and root radius of 0.15 mm was machined to a depth of size *a* with the initial notch aspect ratio a/W= 0.5.

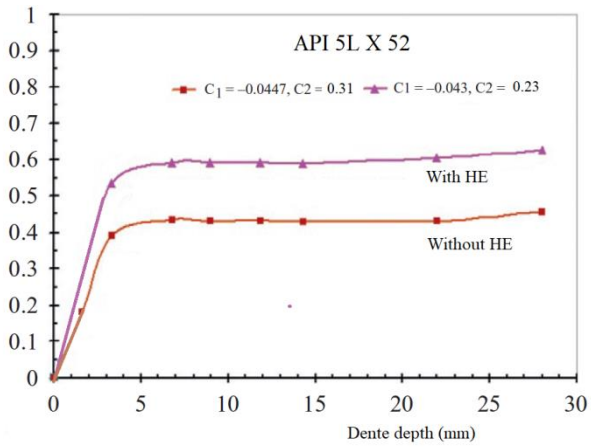

Fig.14: Finite element computation of the integral I (criterion of Oyane) according to the dent depth.

The fatigue initiation resistance curves were entered in figure 15 fitted by a power law:

$$N_i = \sigma_i' \, \Delta\sigma^{\beta} \tag{27}$$

σ_i' is the resistance to fatigue initiation and β an exponent, N_i is the number of fatigue cycles to initiation determined by acoustic emission. The values of σ_i' and β are entered in Table 6.

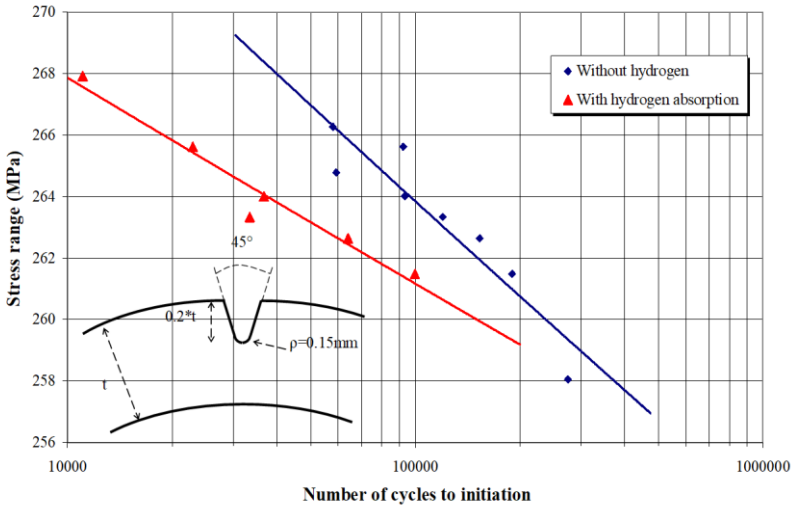

Fig 15: Fatigue initiation resistance curves for pipe steel API 5L X52 with and without HE [24].

We note that the propagation of fatigue cracks is faster in the presence of hydrogen because the N_r-N_i difference is greatly reduced. This difference corresponds to the number of propagation cycles. For this reason, the N_i /N_r ratio is higher in the presence of hydrogen and suffers from a large scatter; N_r is the number of cycles to failure.

Table 6: Fatigue and exponent resistance b for API 5L X52 steel [24].

	Resistance to fatigue initiation $\sigma_i^{'}$ (MPa)	Exponent β	R^2
Without HE	336.05	-0.0202	0.8843
With HE	301.14	-0.0121	0.9502

A global energetic parameter is used as fatigue resistance initiation: the cyclic ΔJ integral [25]. Following the original definition of J-integral for monotonic loading for Cartesian coordinates with the x axis parallel to the crack face and any crack tip encircling contour Γ beginning from the bottom surface of the crack and ending at the top surface, the cyclic J-integral is defined by :

$$\Delta J_{cycl} = \oint_{\Gamma} W^*_{cycl}\, dy - T_{ij}\frac{\partial u}{\partial x}\, ds \tag{28}$$

W^*_{cycl} is the cyclic strain energy density defined by the following relationship:

$$W^*_{cycl} = \int_0^{\Delta\varepsilon} \Delta\sigma_{ij}\, d\varepsilon_{kl} \tag{29}$$

T_{ij} are the surface tensions and u the displacement. It has been proved that this integral is also path independent. The cyclic strain energy density is defined as the area under the ascending branch of the fatigue hysteresis loop. This branch is described by the following power law:

$$\Delta\sigma = K'\Delta\varepsilon^{n'} \tag{30}$$

where K' is the cyclic hardening coefficient and n' the cyclic strain hardening exponent. Fatigue initiation data is fitted according a power law of type:

$$\Delta J_{\rho} = R_{j,i} * N_i^d \tag{31}$$

where ΔJ_{ρ} is the cyclic J range, N_i number of cycles to initiation and d, a constant, figure 16. $R_{J,i}$ is a new parameter named ''Resistance to fatigue initiation''; Values of these parameters are listed in table 7.

Table 7: Values of the parameters of the fatigue initiation resistance curve.

	$R_{J,I}$ (KJ/m2)	d	$\Delta J_{i,th}$ (KJ/m2)
Without hydrogen	2391	-0.991	0.0028
With hydrogen	815	-0.741	0.0026

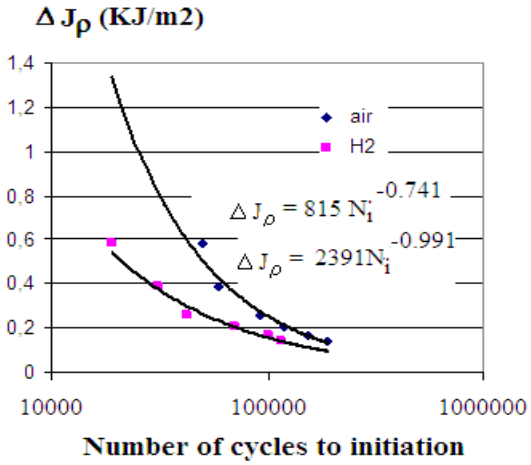

Fig.16: Fatigue initiation curve ΔJρ = f (N_i) for X52 steel.

For a large number of cycles to initiation (1 million for example), we define a conventional fatigue initiation threshold $\Delta J_{i,th}$ .Values of $\Delta J_{i,th}$ are also entered in table 7. These values are helpful to determine if a defect is dormant or not (i.e. non-propagating under cyclic loading).
One notes that for 100,000 cycles fatigue initiation resistance is reduced by 17 %. For a large number of cycles, the fatigue resistance to initiation is similar with and without hydrogen embrittlement. Decreasing of fatigue resistance to initiation by hydrogen absorption is explained for low cycle fatigue by plasticity and interaction of hydrogen and plasticity as can be explained in discussion.
An extension of FAD was recently proposed for fatigue [26], called the fatigue assessment diagram (fAD). In the fAD, the assessment point has coordinates: the non-dimensional load and the applied number of cycles. Basquin's fatigue law is the basis of fAD. When limited to the high cycle fatigue regime, this is:

$$\Delta\sigma = \sigma_{ul} \;\; if \; N \leq N_u$$
$$\Delta\sigma = \sigma_f' N_r^b \; if \;\; N_u < N < N_D$$
$$\Delta\sigma = \sigma_D \;\; if \; N \geq N_D \qquad (32)$$

where is σ_f' the coefficient of Basquin's law, and b Basquin's exponent. N_r is the number of cycles to failure, N_u the number of cycles ($N_u = 10^4$ cycles) for the low cycle fatigue limit and N_D the number of cycles for the endurance domain ($N_D = 10^7$ cycles) for $\Delta\sigma = \sigma_D$ the endurance limit. The fatigue parameter f_r represents the logarithm of the number of cycles to failure. f_r is a function of the loading parameter $Pr = \log_{10}(N_R) = f(P_r)$ (33)

The loading parameter Lr is defined as:

$$\left[\frac{(\sigma_{max} - \sigma_{D,max})}{(\sigma_f' - \sigma_{D,max})}.100 = L_r\right] \qquad (34).$$

The conventional number of cycles that defines the endurance limit is $N_D = 10^7$. $\sigma_{D,max}$, the maximum stress of the cycle at the endurance limit is related to the endurance limit by the ratio of stress R:

$$\sigma_{D,max} = \sigma_D/(1 - R) \quad (35)$$

The choice of the maximum stress as a load parameter is justified by the fact that the calculated stress distribution provides this parameter. In a fatigue evaluation diagram (fAD) an operating point O is defined by its coordinates:

$$L_r = L_r^*$$
$$f_r = f_r^* \quad (36)$$

If the evaluation point is less than the fatigue assessment curve, the component or structure is safe. If the evaluation point is located on the fatigue assessment curve, fatigue failure will occur.

For a given lifetime, the load reduction due to the presence of hydrogen is given by the ratio OB-OA / OB , figure 17.

Table 8 gives the values of the number of cycles to failure for air and hydrogen fatigue tests performed on API 5L X52 steel and the safety factor f_s to be combined if the probability of failure is to be limited to that of the mean minus 3 standard deviations with a coefficient of variation close to CV = 0.1 [26].

Table 8: values of the number of cycles to failure for air and hydrogen fatigue tests carried out on API 5L X52 steel [26]

	Air	H2
Δσ (MPa)	260	260
N_r	$3.28.10^5$	$1.87.10^5$
f_s	1. 43	1.41

It can be seen that hydrogen embrittlement has little effect on fatigue endurance. The value of the working pressures currently used leads pipes subjected to pressure fluctuations to work in fatigue in the field of endurance despite a high stress ratio.

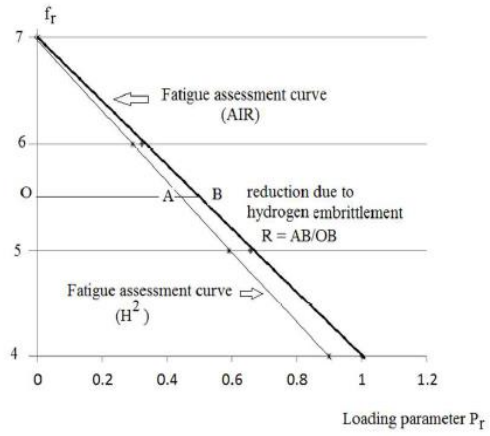

Fig. 17: Influence of hydrogen on the fatigue strength of API 5L X52 pipe steel presented in fAD [26].

7. DISCUSSION

7.1 Calculation of the maximum admissible working pressure (MAWP) for hydrogen transportation

The principle of calculation of the maximum admissible working pressure is based on the formula given by the code [27]:

$$\mathrm{MAWP} = \frac{2\mathrm{SE}'(\mathrm{t} - \mathrm{MA})}{\mathrm{D_e} - 2\mathrm{Y_{B31}}(\mathrm{t} - \mathrm{MA})} \tag{37}$$

where S is the permissible membrane stress of the design code applicable to the design temperature,

E ' is the welding joint efficiency and MA the mechanical correction (depth of thread or groove); for threaded components the nominal thread must apply. The coefficient YB31 is a coefficient of the pipe code ASME B31 [27]. This coefficient depends on the temperature. For ferritic steels and a service temperature below 482°C, the YB_{31} coefficient is equal to 0.4. The thickness t must take into account the future FCA corrosion losses.

For pipe steels, the service stress S is given from the steel yield stress designation S_y:

$$S = \frac{S_y}{f_0} \tag{38}$$

where f_0 is a design factor. The design factor f_0 is given by standards with for example NF EN 10208.2 [28].

The overall risk is therefore the product of all the risks (per year). It is expressed by the probability that a point located near a pipe may be exposed to an intensity greater than a reference level of effect. This probability is expressed by:

$$\Pr(\mathrm{Risk}) = \Pr(\mathrm{F}) * C_{rr} * \Pr(\mathrm{Q}) * \Pr(\mathrm{I}) * \Pr(\mathrm{EF}) * \mathrm{L} * C_{ev} * \Pr(\mathrm{pers}) \tag{39}$$

Pr (F) probability of a leak after rupture,
Pr (Q) probability of flow greater than a threshold,
Pr (I) probability of ignition,
Pr (EF) probability of lethal effects,
Pr (pers) probability of the presence of a person,
L The length of the pipe taken into account,
C_{ev} coefficient to take into account the environment of the pipeline,
C_{rr} risk reduction factor taking into account risk reduction measures.
C_{rr} and C_{ev} are given in the GESIP guidance document [29].

In a conservative manner, risk probability is taken as failure probability. This assumption means that gas flow is larger than the flammability threshold, ignition is immediate, a person is located near the pipe leak and lethal effects are greater than the threshold.
One assumes that the yield stress of pipe steels is distributed according to the 2-parameter Weibull law with m_w the Weibull modulus.

According to [30], the safety factor is related to the probability of survival P_s by the following formula:

$$f_s = \frac{\Gamma_a(1 + 1/m_W)}{[Ln(1/P_s)]^{1/m_W}} \tag{40}$$

Γ_a is the Euler Gamma function. The use of the formula (40) makes it possible to see the values of safety factors for the two conventional values of probability of failure P_r that are usually used ($P_r = 10^{-4}$ if there is no risk to human life, $P_r = 10^{-6}$ if there is this risk. Generally, scatter of steel yield stress is very low and can be evaluated through the Weibull modulus value which is situated in the range [25-40]. Capelle at al [24] noted that the number of cycles to fatigue exhibits a large scatter under HE. For steel yield stress under HE, a low value of m_w =10 is expected;
The values of design factor and associated safety factor are entered in table 9 for two values of the Weibull modulus 10 and 40 and two conventional probabilities of failure.

Table 9: Values of design factor f_0 [28] and associated safety factor fs for 2 values of Weibull modulus 10 and 40 and two conventional probabilities of failure.

Conditions	Design factor f_0	Safety factor f_s
m_w =10 P_r =10^{-4}	0.41	2.38
m_w =10 P_r =10^{-6}	0.26	3.78
m_w = 40 P_r =10^{-4}	0.80	1.24
m_w = 40P_r =10^{-6}	0.71	1.39

Therefore in order to take into account the increase of scatter of yield stress due to HE, the design factor needs to be greatly reduced. Table 10 indicates that the design factor actually used for the design of pipe used for the transport of natural gas [28] cannot ensure a risk probability less than 10-5 in any location of a pipe under HE.

Table 10: Values of the design factor f_0 the risk factor R_s and the risk probability for transport of HE.

Location	Design factor f_0	No-risk factor R_s	Risk probability
country	0.73	1.37	2.60E-02

Semi-urban	0.6	1.67	4.00E-03
Urban	0.4	2.5	7.00E-05

7.2 Recategorization of the defect assessment tool after hydrogen embrittlement

In the FAD, the loading path is linear because the two non-dimensional parameters k_r and L_r are proportional to applied gross stress σ_g if the linear elasticity assumption is used. The angle between this loading path and the L_r axis is called the assessment angle θ. Two particular values of the assessment angle can be defined θ_1 ,θ_2. These two angles determine three failure domains in the Domain Failure Assessment Diagram (DFAD) (Figure.18), (*i*) if $\theta < \theta_1$, localized brittle fracture, (*ii*) if $\theta_1 < \theta < \theta_2$ an elastoplastic fracture zone appears and (*iii*) if $\theta > \theta_2$ plastic collapse.

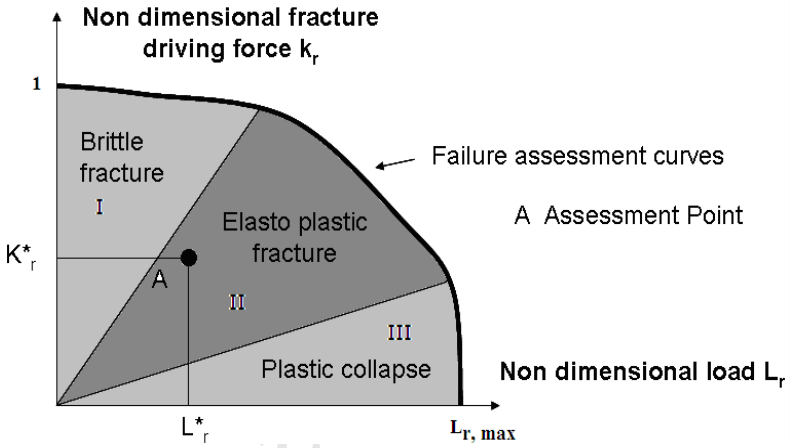

Fig.18. Domain failure assessment diagram with three fracture domains.

Based on Federsen diagram [31] the limit of these three zones is defined conventionally as follows:

$$\begin{aligned} &\text{Zone I} \quad 0 < L_r < 0.62\, L_{r,y} \\ &\text{Zone II} \quad 0.62\, L_{r,y} < L_r < 0.95\, L_{r,L} \\ &\text{Zone III} \quad 0.95\, L_{r,\max} < L_r < L_{r,\max} \end{aligned} \tag{41}$$

where $L_{r,y}$ is associated with the yield pressure and $L_{r,max}$ is the cut-off value. The use of NFAD is particularly interesting to choose the appropriate tool for assessing the risk of failure emanating from a pipe defect. Assessment points are sorted in 3 categories: limit analysis (LA), elasto-plastic fracture mechanics (EPFM) and brittle fracture (BF) according to the DFAD principle. The following criterion was applied:

$$k_r^* \le \mathrm{tg}(\theta_1) L_r^* \rightarrow \mathrm{BF}$$

$$k_r^* \le \mathrm{tg}(\theta_1) L_r^* < \mathrm{tg}(\theta_2) L_r^* \rightarrow \mathrm{EPFM}$$

$$k_r^* \leq tg(\theta_2) L_r^* \rightarrow LA \quad (42)$$

Here we consider a pipe submitted to internal pressure, this pipe is made from API 5L X52 steel. The pipe has a diameter D=611 mm and thickness t = 11 mm and exhibits an internal semi-elliptical crack with aspect ratio a/c = 0.5 and relative crack depth a/t = 0.5. where a is crack depth, t thickness and 2c crack length. True stress/strain of API 5L X52 pipeline steel with and without HE is used to compute J integral applied and the non/dimensional crack driving force is defined as

$$k_r^* = \sqrt{J_{ap} / J_{mat}} \quad (43)$$

where J_{ap}, *is* the applied *J* integral and J_{mat} the material fracture toughness in terms of critical values of *J* Integral. The loading path is entered in figure 19 for both cases with and without HE. One notes that for without HE, the defect assessment (for a relative crack depth a/t = 0.1) is situated in the limit analysis domain. For defect in a pipe submitted to HE, it has to be done according to the LEFM domain. In figure 8, each defect assessment is related only to LEFM.

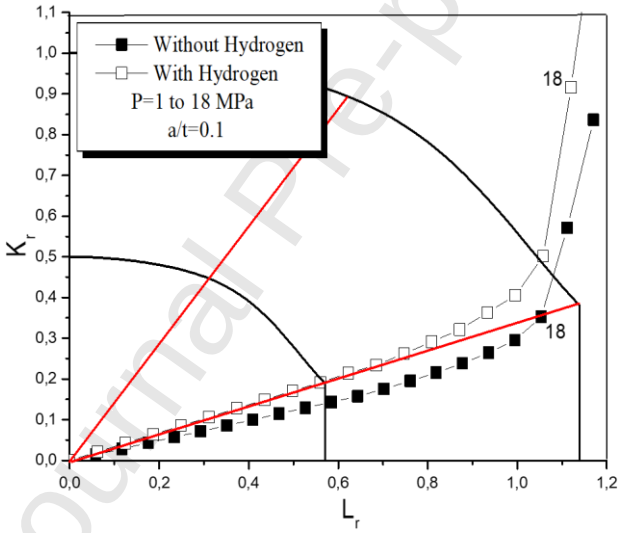

Fig.19: Modification of loading path under HE; pipe submitted to internal pressure made from API 5L X52 steel. Pipe diameter D =611 mm and thickness t=11 mm, relative defect depth a/t =0.1.

The safety factor was obtained using equation 7 in the LEFM domain:

$$f_{s,LEFM} = OC/OB \quad (44)$$

And for the limit analysis domain as:

$$f_{s,LA} = p_s / p_l \quad (45)$$

where p_s is the working pressure and p_l the limit pressure (according to ASME B31 [32]).

Table 11 - Safety factor (f_s) values for different relative crack depths ratios (a/t=0.1 to 0.5), with and without hydrogen and for different gas pressures (p =5 MPa and 11 MPa).

f_s	p_{ap}=5 MPa			p_{ap}=11 MPa		
a/t	Without HE (EPFM)	Without HE (LA)	With HE (EPFM)	Without H_2 (EPFM)	Without HE (LA)	With H_2 (EPFM)
0.1	-	3.47 (3.85)	3.70	-	1.58 (1.79)	1.67
0.2	-	3.47 (3.45)	3.23	-	1.58 (1.56)	1.47
0.3	-	3.47 (3.03)	2.78	-	1.58 (1.37)	1.27
0.4	2.63	-	2.33	1.18	-	1.04
0.5	2.17	-	2.00	0.98	-	0.89

Values of safety factor according to the previous definitions are entered in table 11 s for different relative defect depth-ratios (a/t=0.1 to 0.5), with and without HE and for 2 different gas pressures. Fs, LA was calculated for the relative defect depth a/t =0.1; 0.2 and 0.3 where the loading path is situated in the LA domain of the DFAD. Corresponding values for LEFM analysis are entered in brackets. One notes that the safety factors decrease when the applied pressure increases. Decreases after HE are less than 10%. When the relative defect depth increases, the safety factor associated with LA is greater than the LEFM one.

With HE	109.5	57	0.087	0.012	1.68 e+4

CONCLUSION

For safety reasons the transport of pure hydrogen or natural gas and hydrogen blend in pipe networks made of steel needs to take into account hydrogen embrittlement. This phenomenon due to weakening of metal-metal atomic bonds and modification of plasticity is characterized by detrimental effects on mechanical properties. However the different mechanical properties are not affected with the same intensity. Yield stress, ultimate strength and fatigue endurance limit are little affected. On the other hand, elongation at failure, fracture toughness and resistance to fatigue crack propagation are greatly reduced. These effects need to be taken into account in pipe design and maintenance.

Maximum allowable working pressure depends on the yield stress designation which is not affected by HE. However, steel's mechanical properties suffer, after HE, of larger scatter associated with scatter of hydrogen traps. This needs to be taken into account for safe probabilistic design through the design factor. Risk probabilities are expected to be lower than 10^{-4} in country and 10^{-5} for urban location according to API.

Pipe defect assessment needs specific tools for each defect type (crack, gouge, corrosion crater or dente). These tools use flow stress (little sensitive to HE), fracture toughness or elongation at failure (very sensitive to HE). Therefore pipe defect assessment needs to know a large variety of mechanical properties under HE and it is conservative to apply in any case a reduction of the working pressure.

Maintenance policy needs to pay attention to defect size in order to guaranty a minimum safety factor. *HE has a strong influence on the time between inspections for two reasons: admissible defect size is strongly reduced due the decrease of fracture toughness and defect growth under fatigue is accelerated under HE.*

The introduction of pure hydrogen or blending natural gas and hydrogen in steel pipes needs design and maintenance using the same tools as in the case of transport of natural gas. However, it needs good data of mechanical properties under HE with precise experimental conditions particularly hydrogen absorption pressure which has to be close to working pressure, because HE increase with hydrogen pressure.

Probabilistic design is necessary to evaluate risk after hydrogen introduction and needs scatter description. This leads to consider new values of the design factor.

References

[1] W. H. Johnson: Proceedings of the Royal Society of London, 23:168–179, (1875).
[2] J. Capelle, I. Dmytrakh, G. Pluvinage "Electrochemical hydrogen absorption of API X52 steel and its effect on local fracture emanating from notches". Journal of Structural integrity and Life , Vol.9, N°1: 3-8 (2009).
[3] API 579-1 / ASME FFS-1 2007 Fitness-Pour-Service 7-13 section 9, (2009).
[4] Thompson A.W."Stress Corrosion Cracking and Hydrogen Embrittlement". Metallurgical Treatises; Metallurgical Society : 589-601; P. A. (1985).
[5] NewmanJ.C, Raju I.S,"Stress intensity factor for internal and external surface cracks in cylindrical pressure vessels". J of Pressure Vessels Technology, vol 104, Nov, (1982).
[6] SINTAP: Structural Integrity Assessment Procedure, Final Report E-U project BE95-1462 Brite Euram Programme Brussels, (1999).
[7] Harrisson R.P , Milne I and Loosmore K "Assessment of the integrity of structures containing defects". Central Electricity Generating Board Report R/H R6 Revision 1 , leatherhzead, surrey, UK, (1977).
[8] RCC-MRx 2015 - EN Design and Construction Rules for mechanical components of nuclear installations : high-temperature, research and fusion reactors, AFCEN, Paris (2015).
[9] L. Briottet , R. Batisse, G. de Dinechin, P. Langlois, L. Thiers. "Recommendations on X80 steel for the design of hydrogen gas transmission pipelines". International Journal o Hydrogen Energy,37 : 9423 -9430, (2012).
[10] American National Standard Institute (ANSI)/American Society of Mechanical Engineers (ASME). Manual for determining strength of corroded pipelines, ASME B31G; 1984.
[11] Kiefner J, Vieth P. "A modified criterion for evaluating the strength of corroded pipe". Final report for PR 3-805 project to the Pipeline Supervisory Committee of the American Gas Association, Battelle, Ohio; (1989).
[12] Recommended Practice, Det Norske Veritas, DNV-RP-F101, Corroded Pipelines, (20049.
[13] Choi J. B , Goo B. K, Kim J. C , Kim Y. J , Kim W. S." Development of limit load solutions for corroded gas pipelines", International Journal of Pressure Vessel and Piping,; 80 (2) :121-128, (2003).

[14] Pluvinage G. "Notch effects in fatigue and Fracture"; Editeur Kluwer, (2001).
[15] H. Elminor, A. Kifani, Z. Azari, M. Louah, G. Pluvinage "Fracture toughness of Strength Steel-Using the notch stress factor and volumetric approach", Structural Safety, Elsevier sciences, (2002).
[16] Larsson S.G and Carlsson A. J "Influence of non-singular stress terms and specimen geometry on small-scale yielding at crack tips in elastic–plastic materials", J Mech Phys Solids, 1, Vol (21): 263–77, (1973).
[17] Yang. B, Ravichandar. K "Evaluation of T stress by stress difference method". Engng Fract Mech,; Vol 64 :589–605, (2001).
[18] Hadj Meliani M, MatvienkoY. G, Pluvinage G. "Two-parameter fracture criterion ($K_{\rho,c}$-$T_{ef,c}$) based on notch fracture mechanics", Inter. Journal of Fracture Vol 167 : 173–182, (2011).
[19] O. Bouledroua1, M. Hadj Meliani and G. Pluvinage,"Assessment of pipe defects using a constraint modified failure assessment diagram" Journal of Failure Analysis and Prevention, Volume 17, Issue 1, pp 144–153 February, (2017). [20] Eiber RJ. "The effect of dents on the failure characteristics of linepipe", Batelle Colombus Laboratories, NG 18, Report no. 125; May,(1981).
[21] Jones DG. "The significance of mechanical damage in pipelines". 3R International, 21, Jahrgang, Heft; (1982).
[22] 7th Report of European Gas Pipeline Incident Data Group, 1970–2007, Gas pipeline Incidents :1–33 –December (2008).
[23] M. Oyane, T.Sato, K. Okimoto, S. Shima, "Criteria for ductile fracture and their application", J. Mech. Work technol. 4, (1980).
[24]. J. Capelle, J. Gilgert, G. Pluvinage;"A fatigue initiation parameter for gas pipe steel submitted to hydrogen absorption".International Journal of Hydrogen Energy, Volume 35, Issue 2, January : 833-843, (2010).
[25] J. Capelle, J. Predan, N. Gubeljak, G. Pluvinage, "The use of cyclic ΔJ_ρ as a parameter for fatigue initiation of X52 steel Engineering Fracture Mechanics, Volume 96 :82-95, (2012).
[26] S Jallouf , J. Capelle and G Pluvinage "Probabilistic fatigue initiation assessment diagram for pipe steel X 52: influence of hydrogen".Fatigue & Fracture of Engineering Materials & Structures, Volume 40, Issue 8 :1260-1266, (2017).
[27] ASME B31.1 Power piping ,(2016).
[28] Arrêté du 4 aout 2006 portant sur le règlement de la sécurité des canalisations de transport de gaz combustibles, d'hydrocarbures liquides ou liquéfiés et de produits chimiques. Fr J Officiel (2006).
[29] GESIP, Rapport n°2008/01, "Guide Méthodologique pour la réalisation d'une étude de sécurité concernant une canalisation de transport (hydrocarbures liquides ou liquéfiés, gaz combustibles et produits chimiques) ", décembre (2008).
[30] G Pluvinage et V.Sapounov -"Prévision statistique du comportement des matériaux". Editeur CEPADUES, (2006).
[31] Feddersen C.E "evaluation and prediction of residual strength of center cracked tension panels ".ASTM STP 486 : 50-62, (1970).
[32] ASME B31G-2009: Manual for Determining the Remaining Strength of Corroded Pipelines[S]. American Society of Mechanical Engineers, New York, (2009).

[33] HJ Cialone and JH Holbrook“Effects of gaseous hydrogen on fatigue crack growth in pipeline steel”. Metallurgical Transactions A January, Volume 16, Issue 1 : 115–122, (1985).
[34] L. Briottet , R. Batisse, G. de Dinechin, P. Langlois, L. Thiers. “Recommendations on X80 steel for the design of hydrogen gas transmission pipelines”. international Journal o Hydrogen Energy,37 : 9423 -9430, (2012)

ACKNOWLEDGEMENT
Authors thank INERIS for financial support

Highlight

- ✓ **hydrogen embrittlement (HE) is taken into account for the design and maintenance of pipe networks.**
- ✓ **The design needs to modify the design factor for computing the maximum working pressure.**
- ✓ **harmfulness is determined with a failure assessment diagram with steel fracture toughness under the HE effect.**
- ✓ **For defect correction, the estimated repair factor (ERF) is changing due to modification of the flow stress.**
- ✓ **The influence of HE on fatigue endurance is seen through the fatigue assessment diagram (FAD**

I declare that there is no conflict of interest

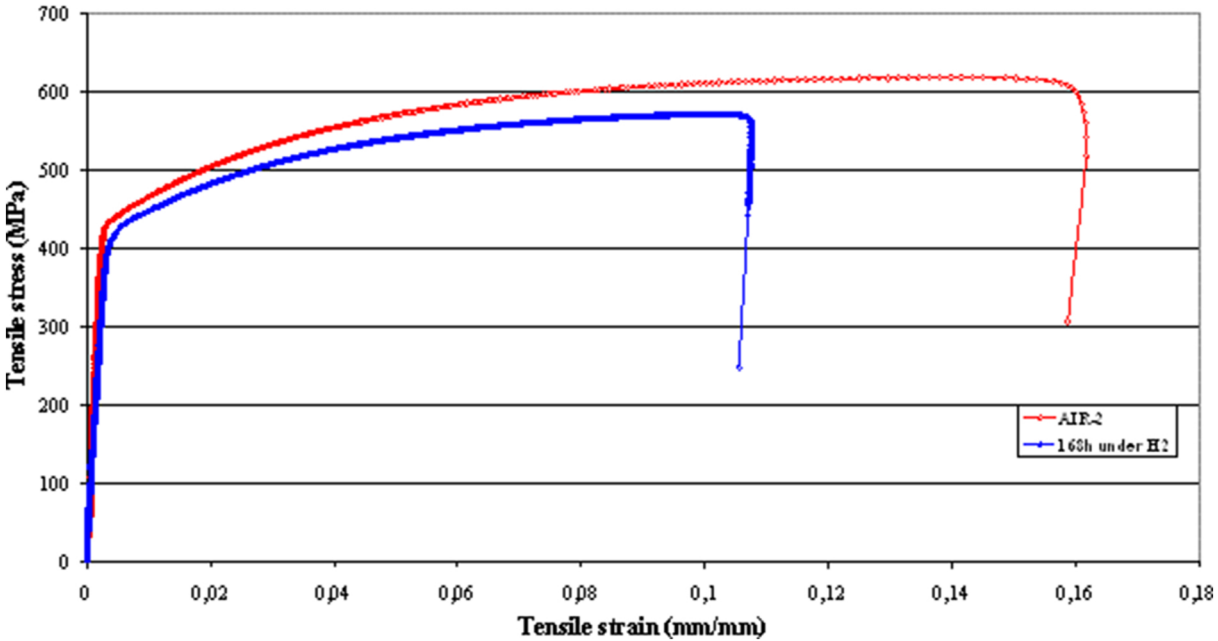
API 5L X52
Tensile stress (MPa)
Tensile strain (mm/mm)
700
600
500
400
300
200
100
0
0
0,02
0,04
0,06
0,08
0,1
0,12
0,14
0,16
0,18
AIR-2
168h under H2

Figure 1

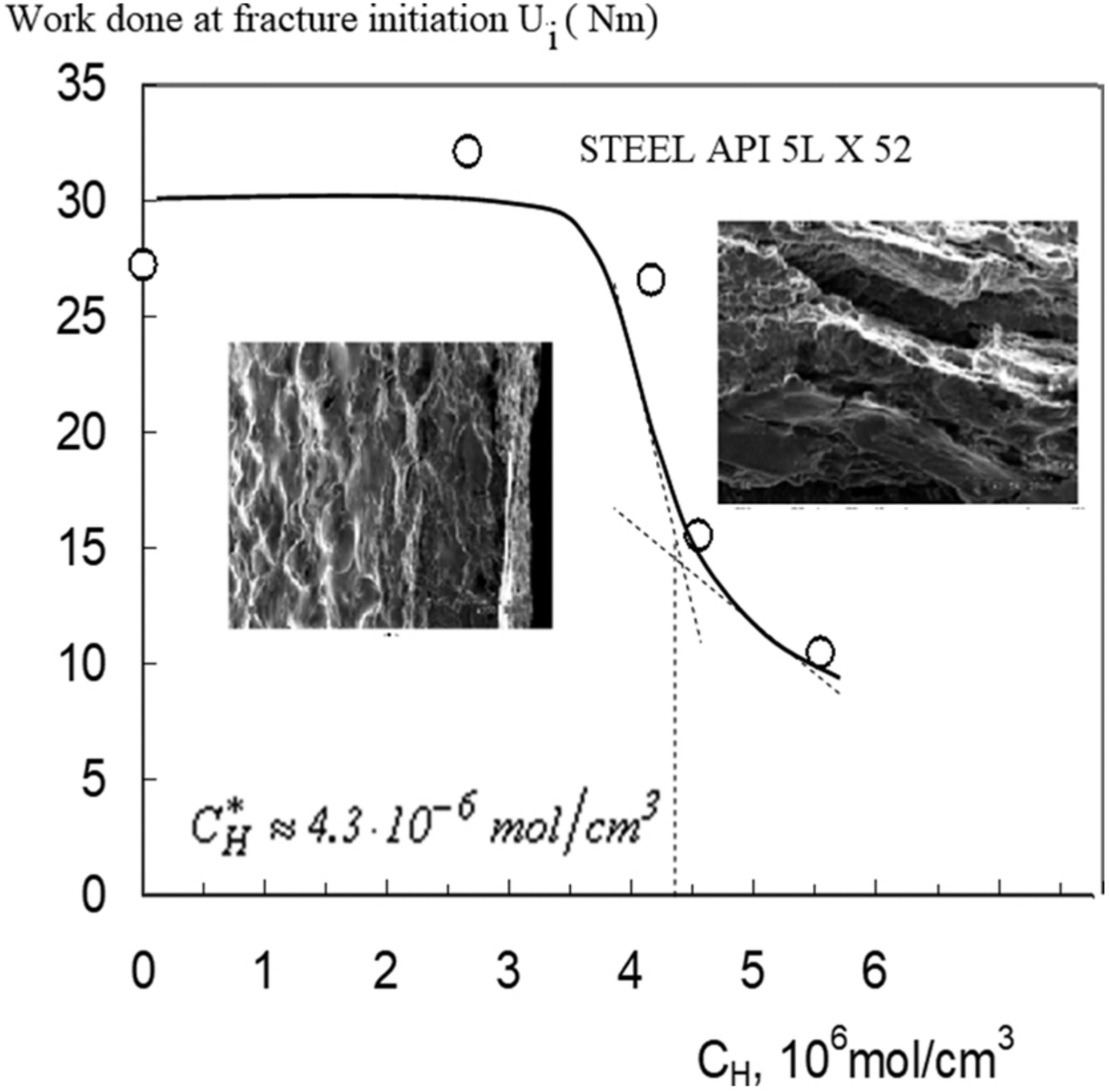
Work done at fracture initiation U_i (Nm)
35
30
25
20
15
10
5
0
STEEL API 5L X 52
$C_H^* \approx 4.3 \cdot 10^{-6}$ mol/cm^3
0
1
2
3
4
5
6
C_H, 10^6mol/cm^3

Figure 2

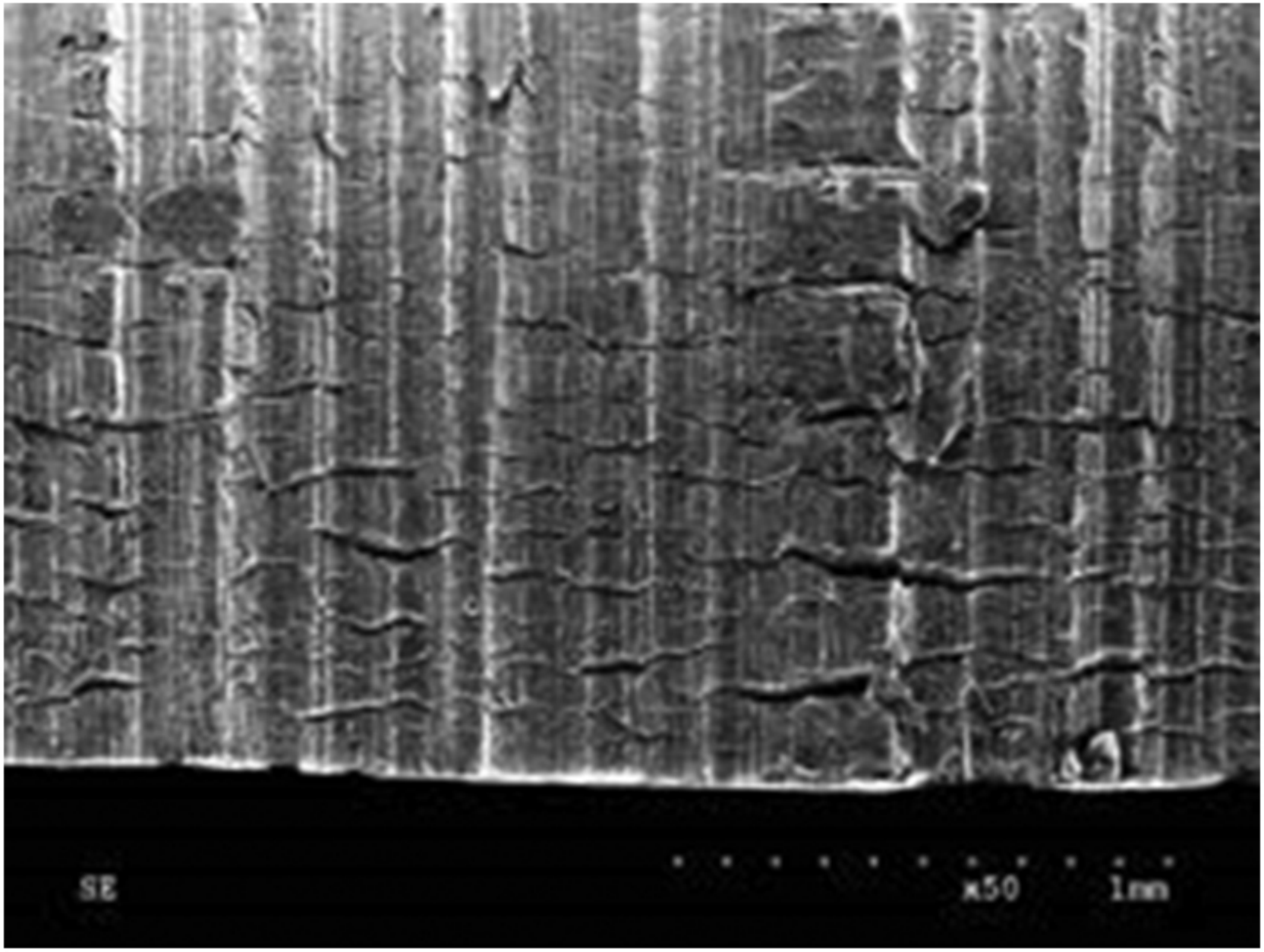

Figure 3

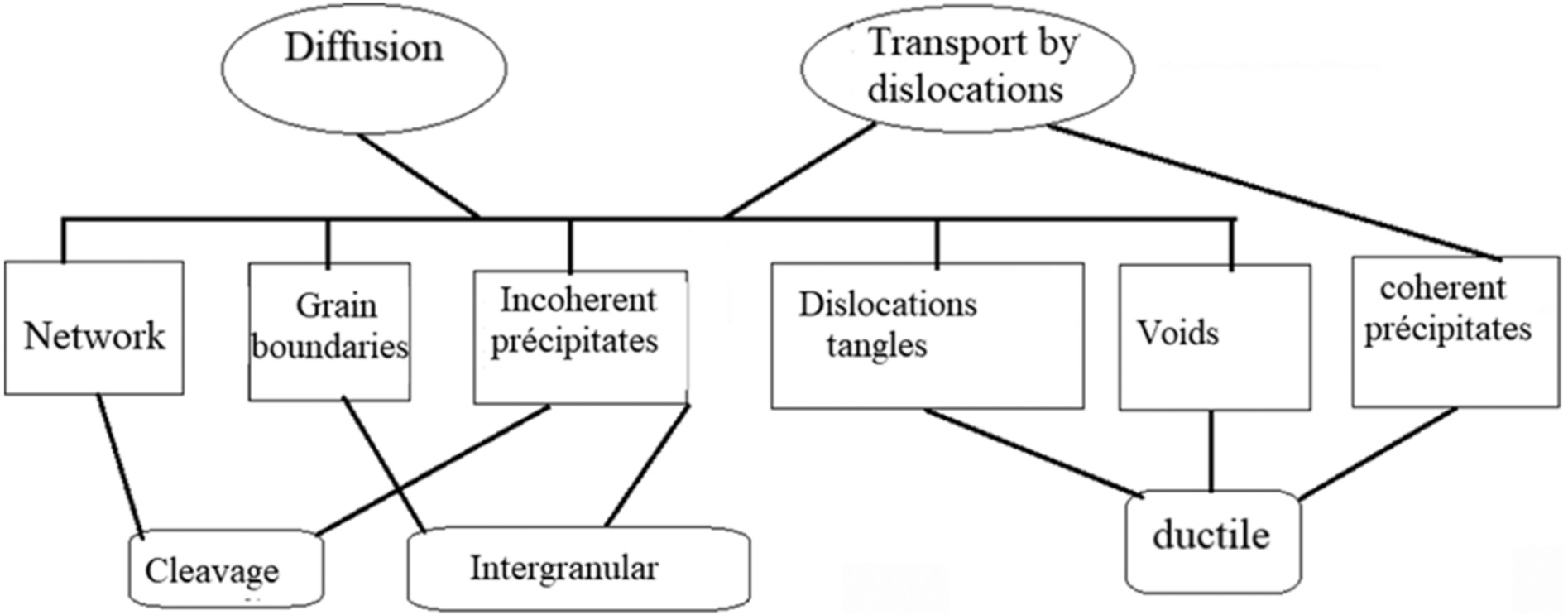
Diffusion
Transport by dislocations
Network
Grain boundaries
Incoherent précipitates
Dislocations tangles
Voids
coherent précipitates
Cleavage
Intergranular
ductile

Figure 4

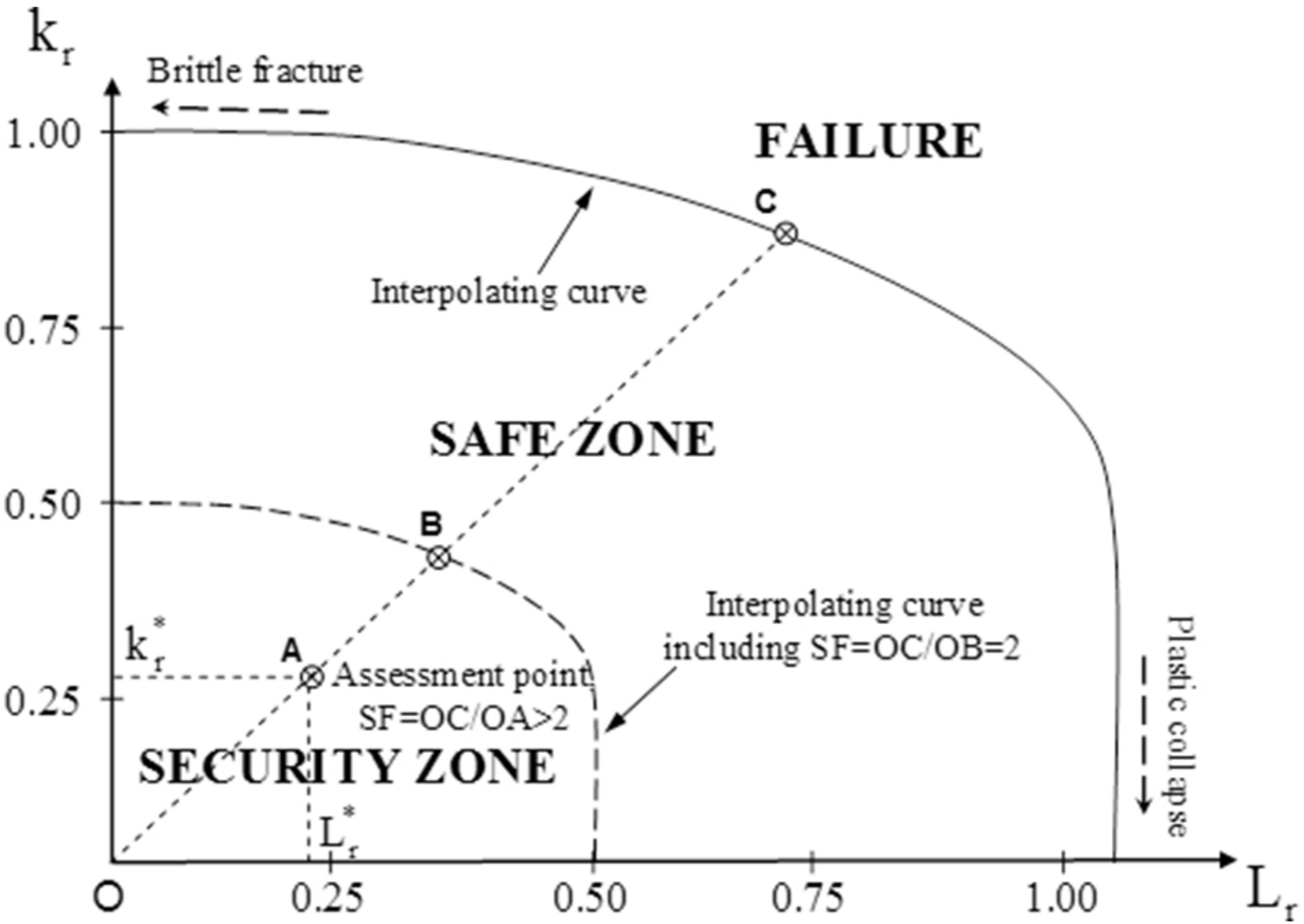
k_r
Brittle fracture
1.00
FAILURE
C
Interpolating curve
0.75
SAFE ZONE
0.50
B
Interpolating curve
including SF=OC/OB=2
k_r^*
A
Assessment point
SF=OC/OA>2
0.25
SECURITY ZONE
L_r^*
Plastic collapse
O
0.25
0.50
0.75
1.00
L_r

Figure 5

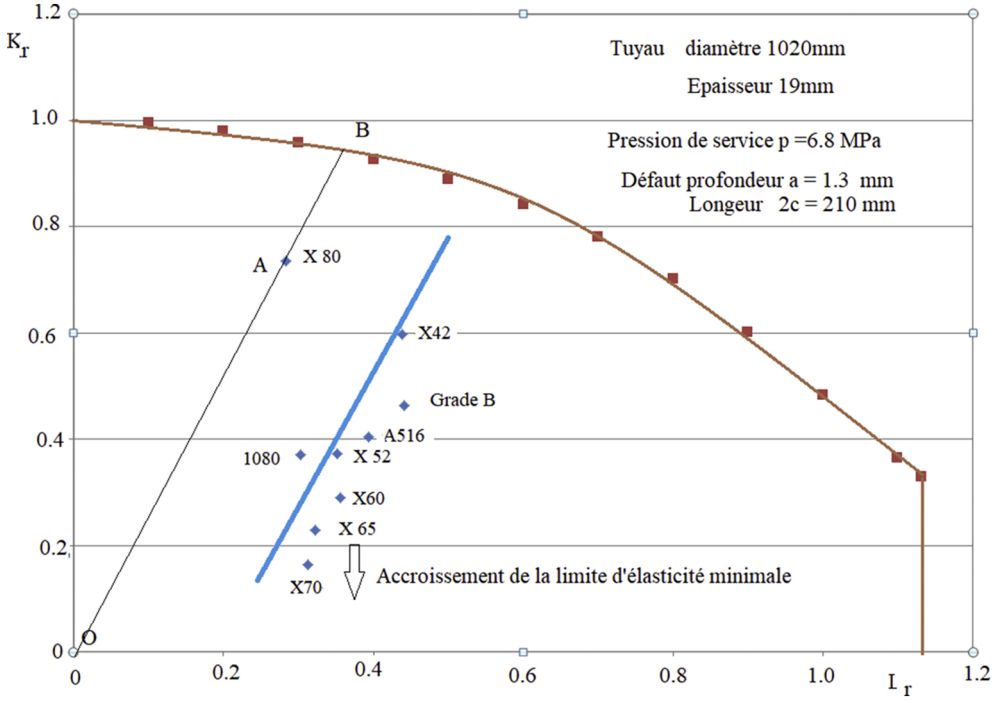
K_r
1.2
1.0
0.8
0.6
0.4
0.2
0
0
0.2
0.4
0.6
0.8
1.0
1.2
I_r
Tuyau diamètre 1020mm
Epaisseur 19mm
Pression de service p =6.8 MPa
Défaut profondeur a = 1.3 mm
Longeur 2c = 210 mm
A
B
O
X 80
X42
Grade B
A516
1080
X 52
X60
X 65
X70
Accroissement de la limite d'élasticité minimale

Figure 6

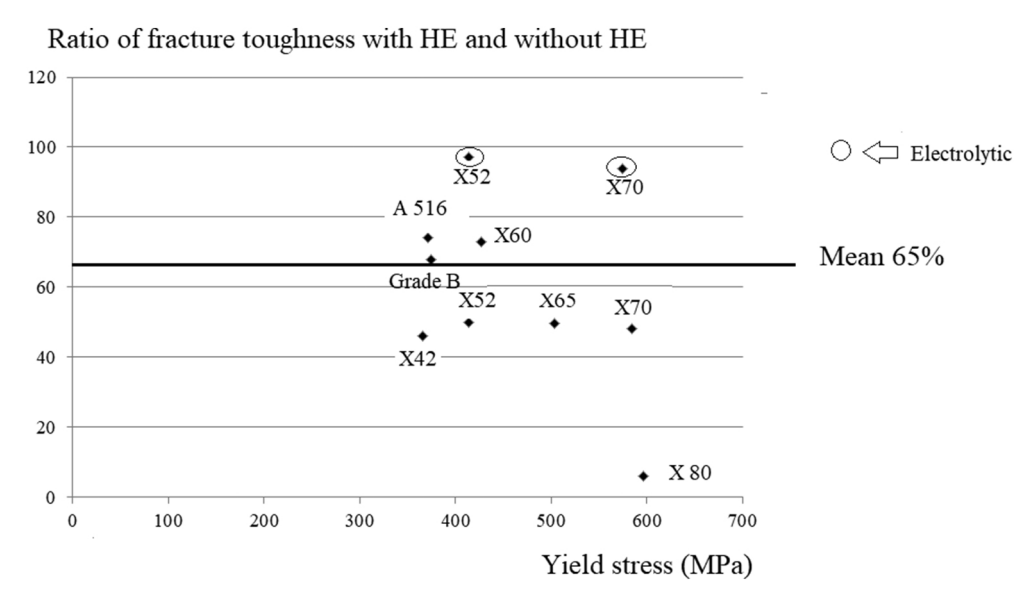
Ratio of fracture toughness with HE and without HE
120
100
80
60
40
20
0
0
100
200
300
400
500
600
700
Yield stress (MPa)
X52
X70
A 516
X60
Grade B
Mean 65%
X52
X65
X70
X42
X 80
Electrolytic

Figure 7

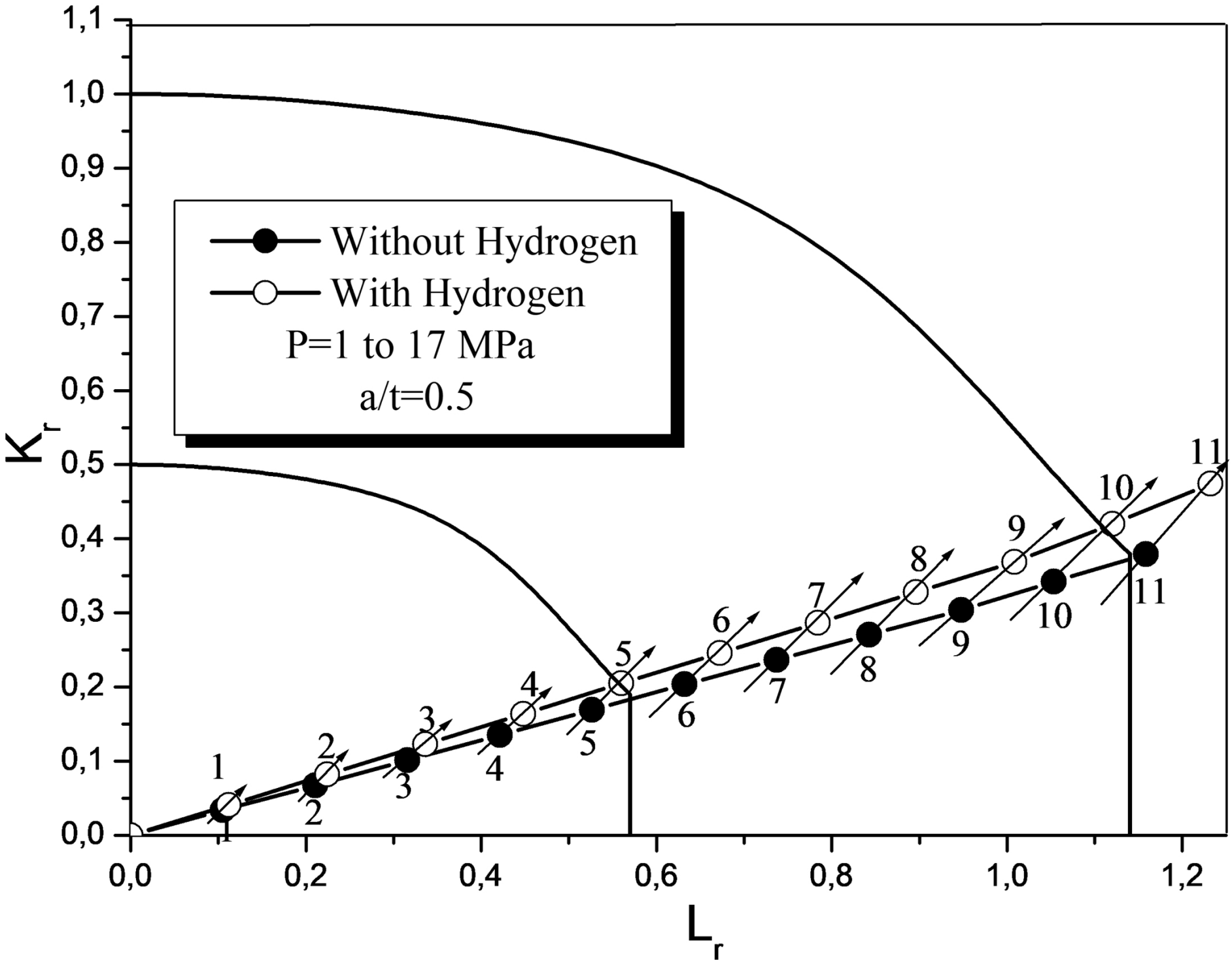
Without Hydrogen
With Hydrogen
P=1 to 17 MPa
a/t=0.5
K_r
L_r
1,1
1,0
0,9
0,8
0,7
0,6
0,5
0,4
0,3
0,2
0,1
0,0
0,0
0,2
0,4
0,6
0,8
1,0
1,2
1
2
3
4
5
6
7
8
9
10
11

Figure 8

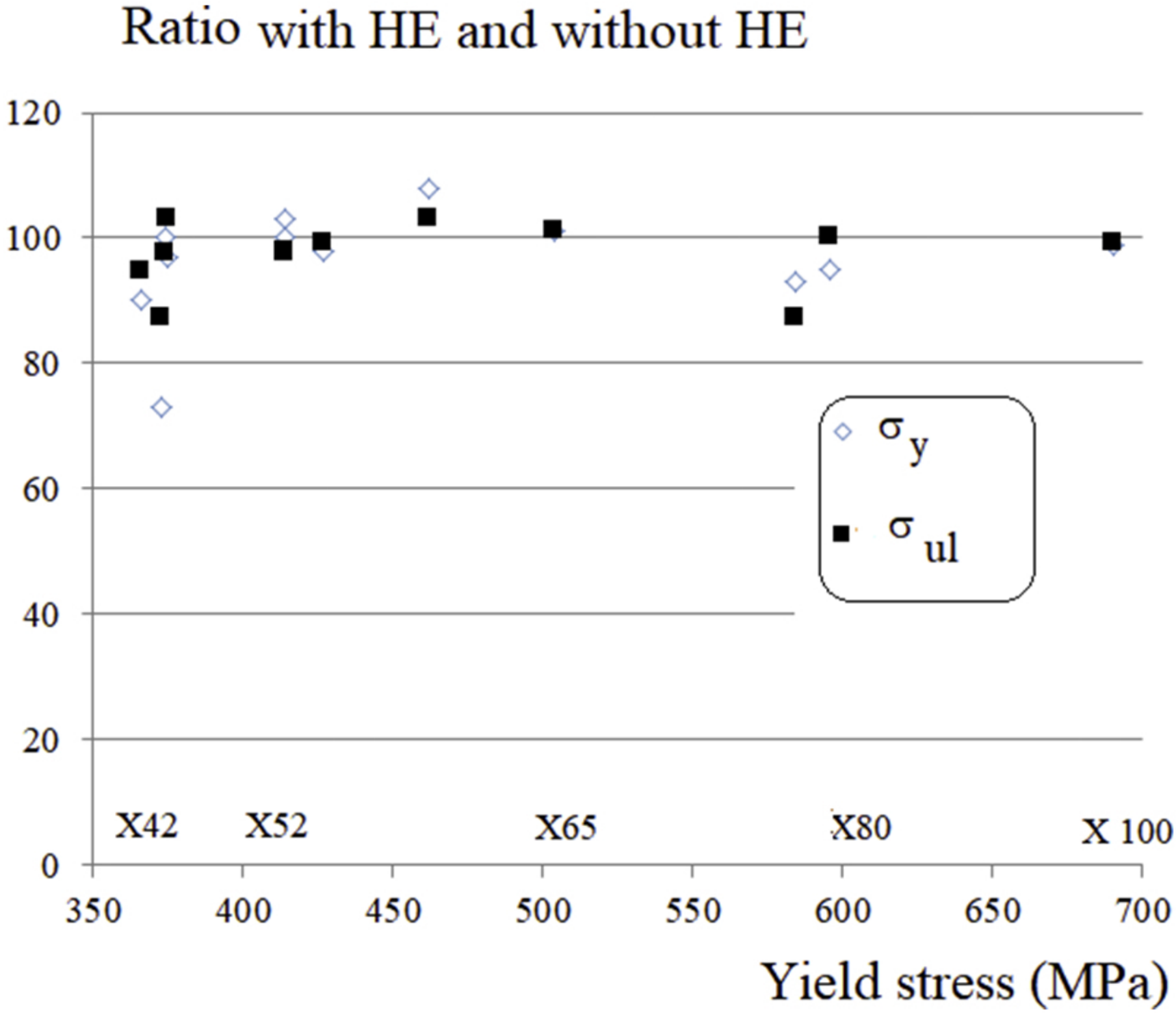
Ratio with HE and without HE
120
100
80
60
40
20
0
σ y
σ ul
X42
X52
X65
X80
X 100
350
400
450
500
550
600
650
700
Yield stress (MPa)

Figure 9

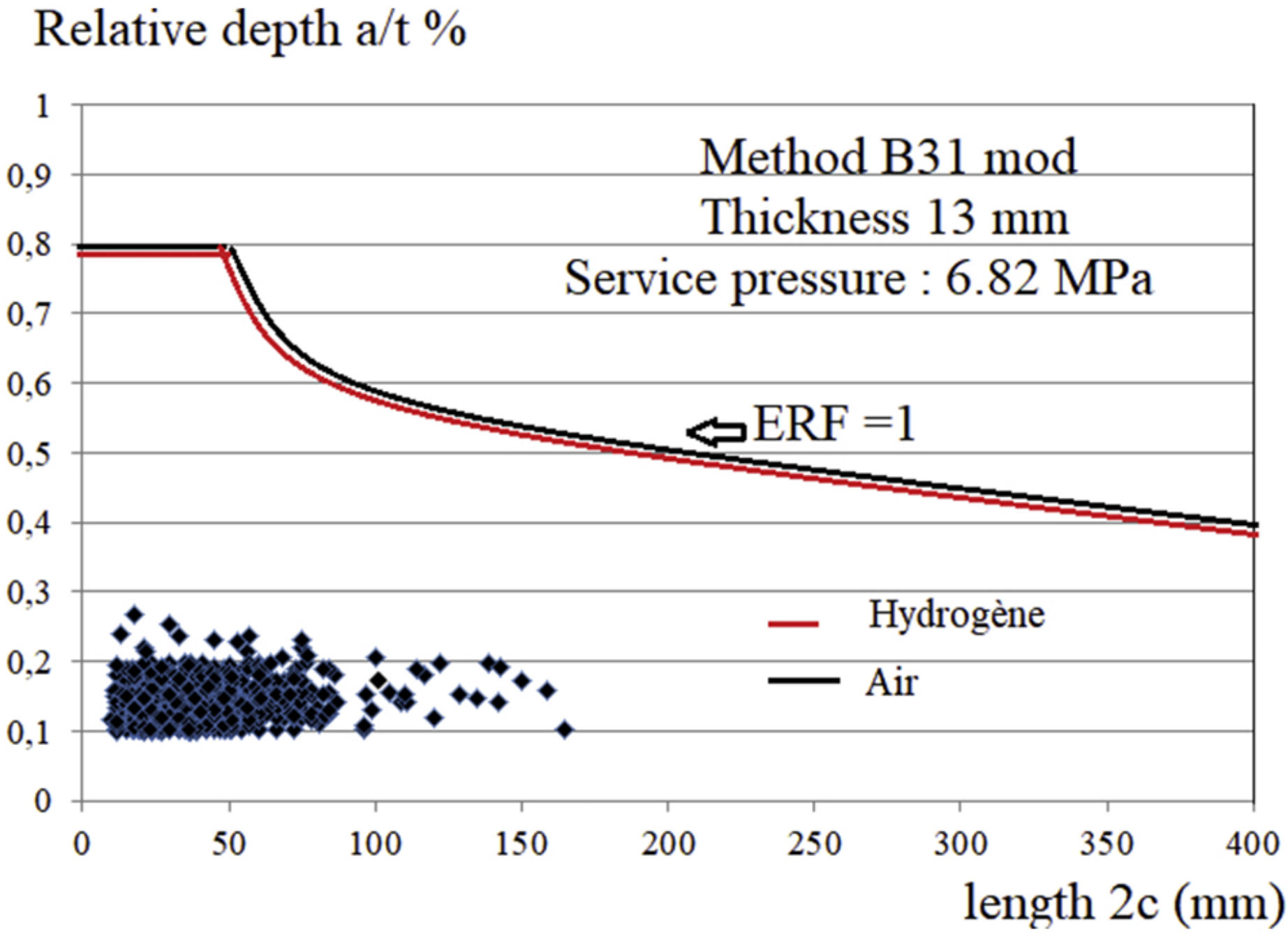
Relative depth a/t %
1
0,9
0,8
0,7
0,6
0,5
0,4
0,3
0,2
0,1
0
Method B31 mod
Thickness 13 mm
Service pressure : 6.82 MPa
ERF =1
Hydrogène
Air
0
50
100
150
200
250
300
350
400
length 2c (mm)

Figure 10

Figure 11

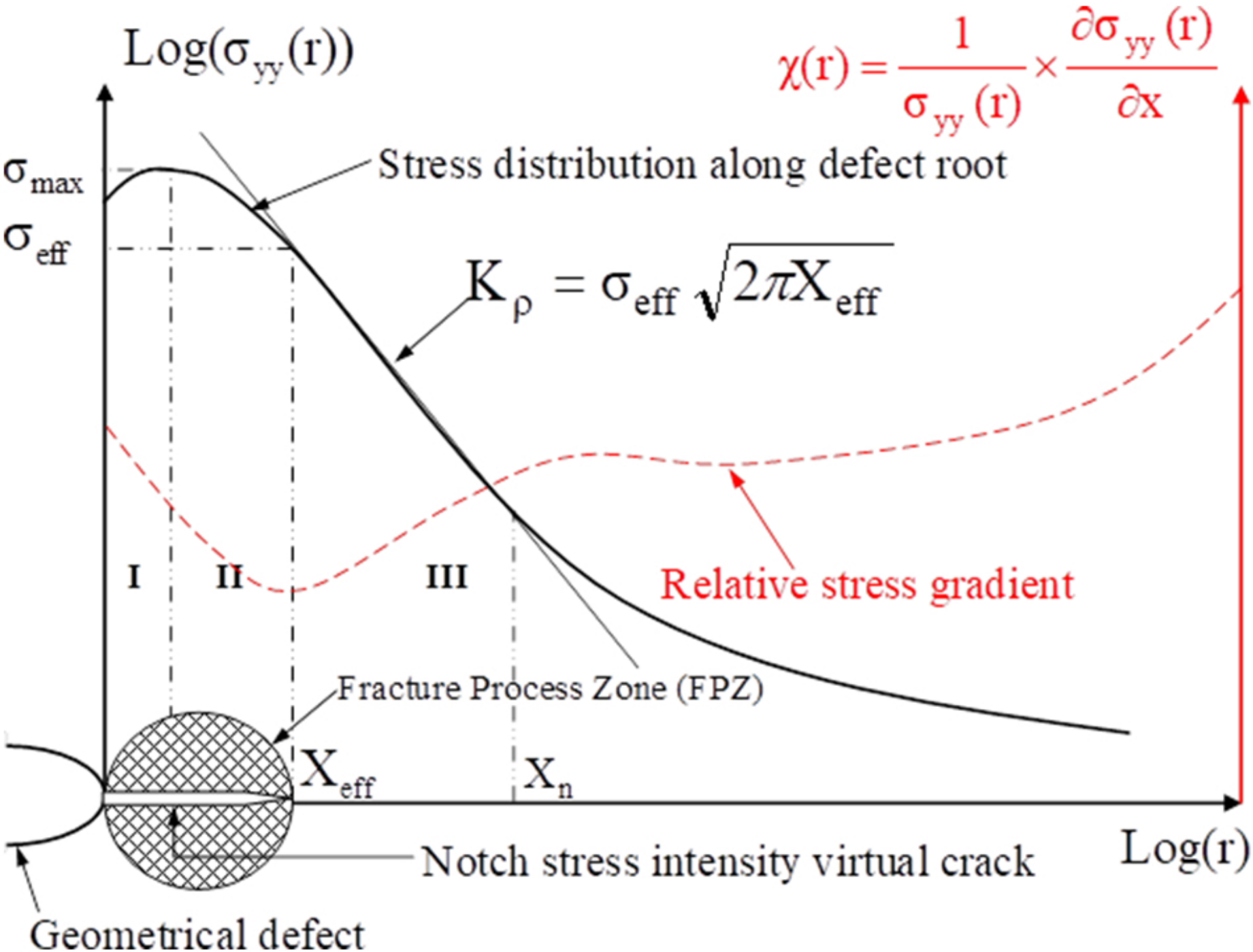
Log(σyy(r))
χ(r) = 1/σyy(r) × ∂σyy(r)/∂x
σmax
σeff
Stress distribution along defect root
Kρ = σeff √(2πXeff)
I
II
III
Relative stress gradient
Fracture Process Zone (FPZ)
Xeff
Xn
Notch stress intensity virtual crack
Log(r)
Geometrical defect

Figure 12

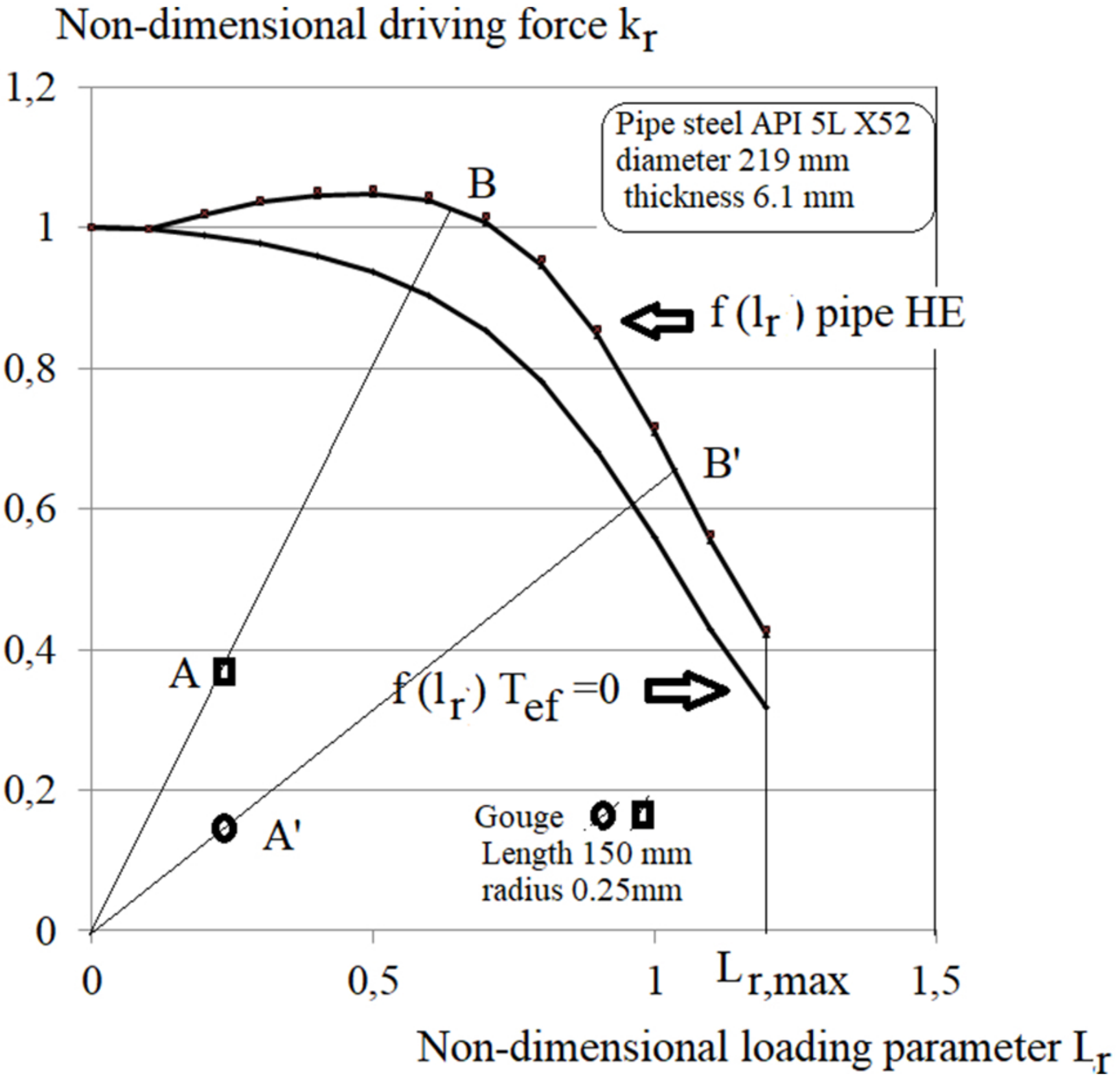
Non-dimensional driving force k_r
1,2
1
0,8
0,6
0,4
0,2
0
Pipe steel API 5L X52
diameter 219 mm
thickness 6.1 mm
B
B'
A
A'
f (l_r) pipe HE
f (l_r) T_{ef} =0
Gouge
Length 150 mm
radius 0.25mm
0
0,5
1
$L_{r,max}$
1,5
Non-dimensional loading parameter L_r

Figure 13

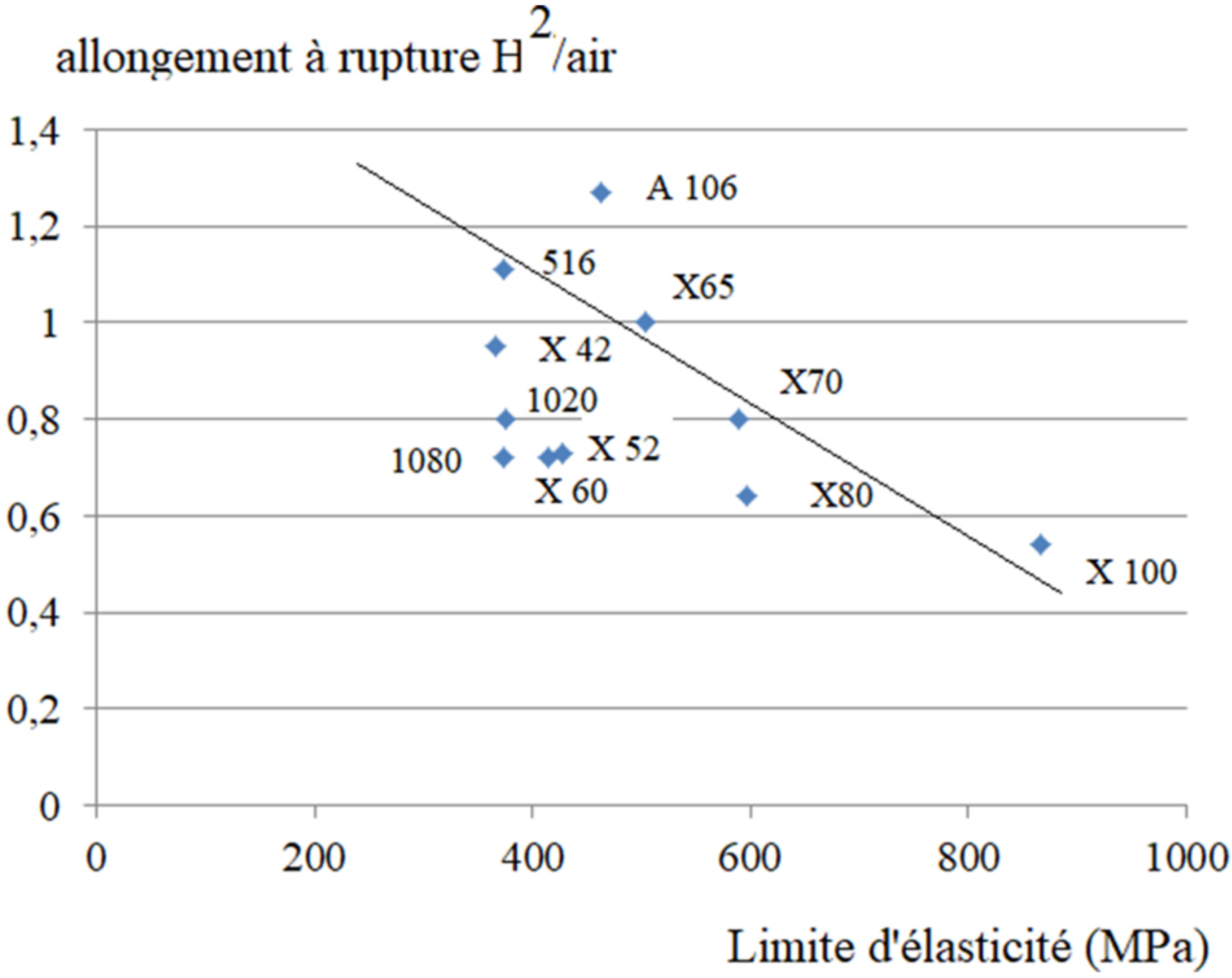
allongement à rupture H2/air
1,4
1,2
1
0,8
0,6
0,4
0,2
0
0
200
400
600
800
1000
Limite d'élasticité (MPa)
A 106
516
X65
X 42
X70
1020
1080
X 52
X 60
X80
X 100

Figure 14

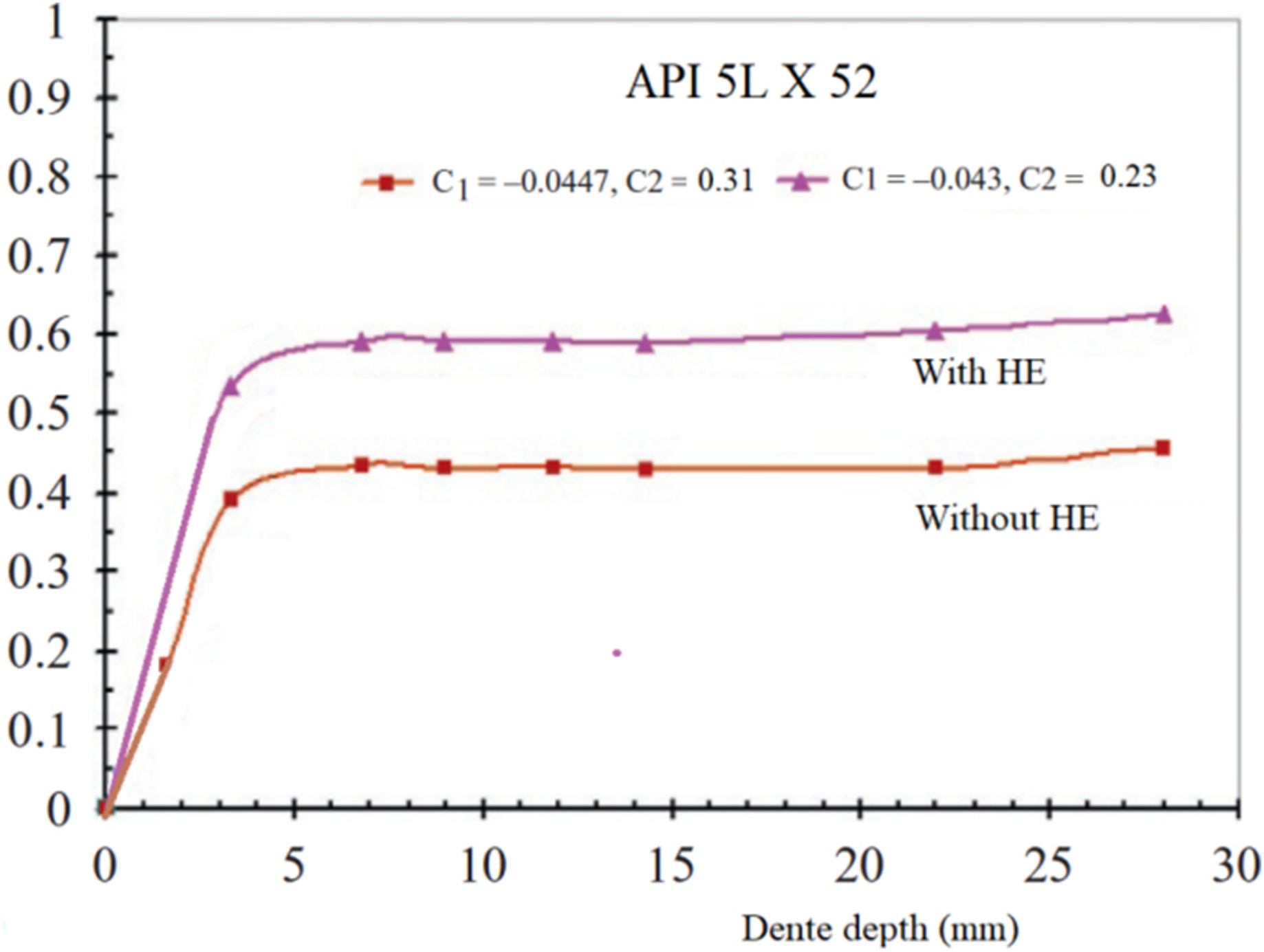
API 5L X 52
C1 = –0.0447, C2 = 0.31
C1 = –0.043, C2 = 0.23
With HE
Without HE
1
0.9
0.8
0.7
0.6
0.5
0.4
0.3
0.2
0.1
0
0
5
10
15
20
25
30
Dente depth (mm)

Figure 15

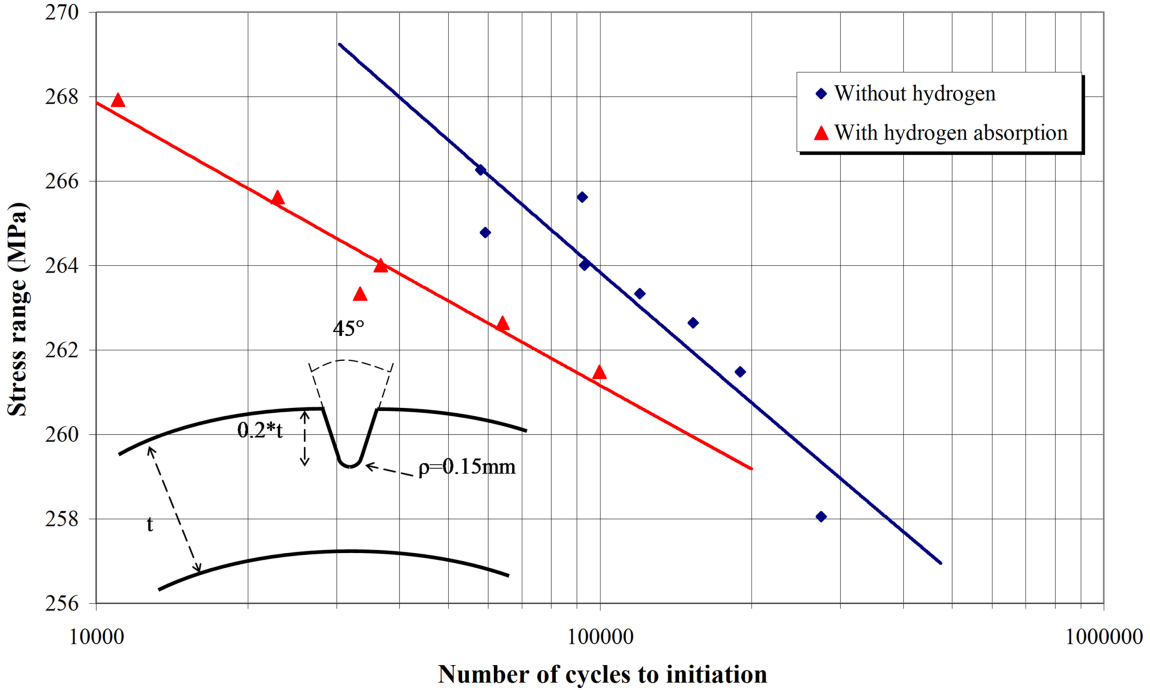
270
268
266
264
262
260
258
256
Stress range (MPa)
10000
100000
1000000
Number of cycles to initiation
Without hydrogen
With hydrogen absorption
45°
0.2*t
ρ=0.15mm
t

Figure 16

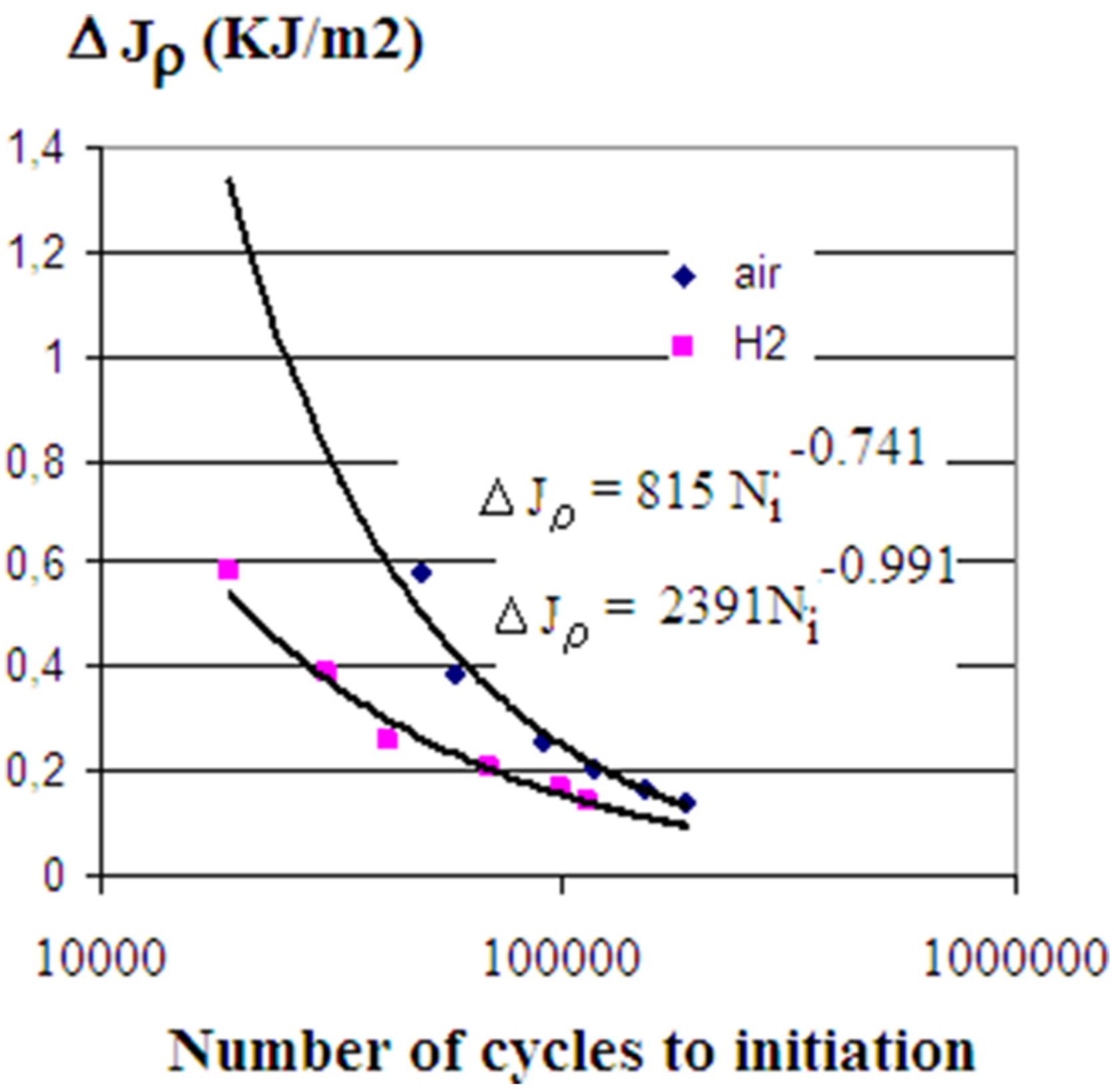
Δ Jρ (KJ/m2)
1,4
1,2
1
0,8
0,6
0,4
0,2
0
air
H2
Δ Jρ = 815 Ni -0.741
Δ Jρ = 2391Ni -0.991
10000
100000
1000000
Number of cycles to initiation

Figure 17

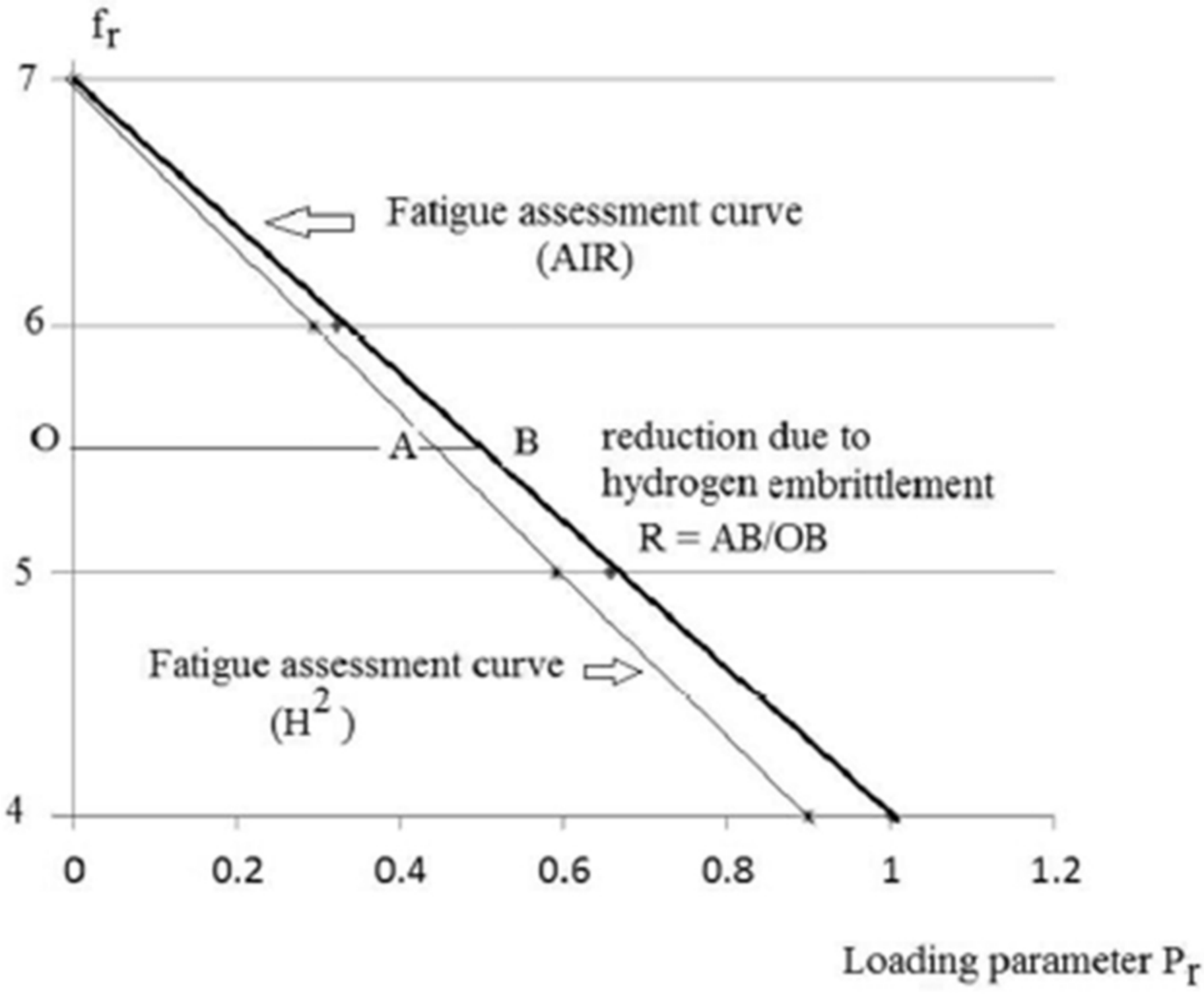
f_r
7
6
O
5
4
A
B
Fatigue assessment curve
(AIR)
reduction due to
hydrogen embrittlement
R = AB/OB
Fatigue assessment curve
(H^2)
0
0.2
0.4
0.6
0.8
1
1.2
Loading parameter P_r

Figure 18

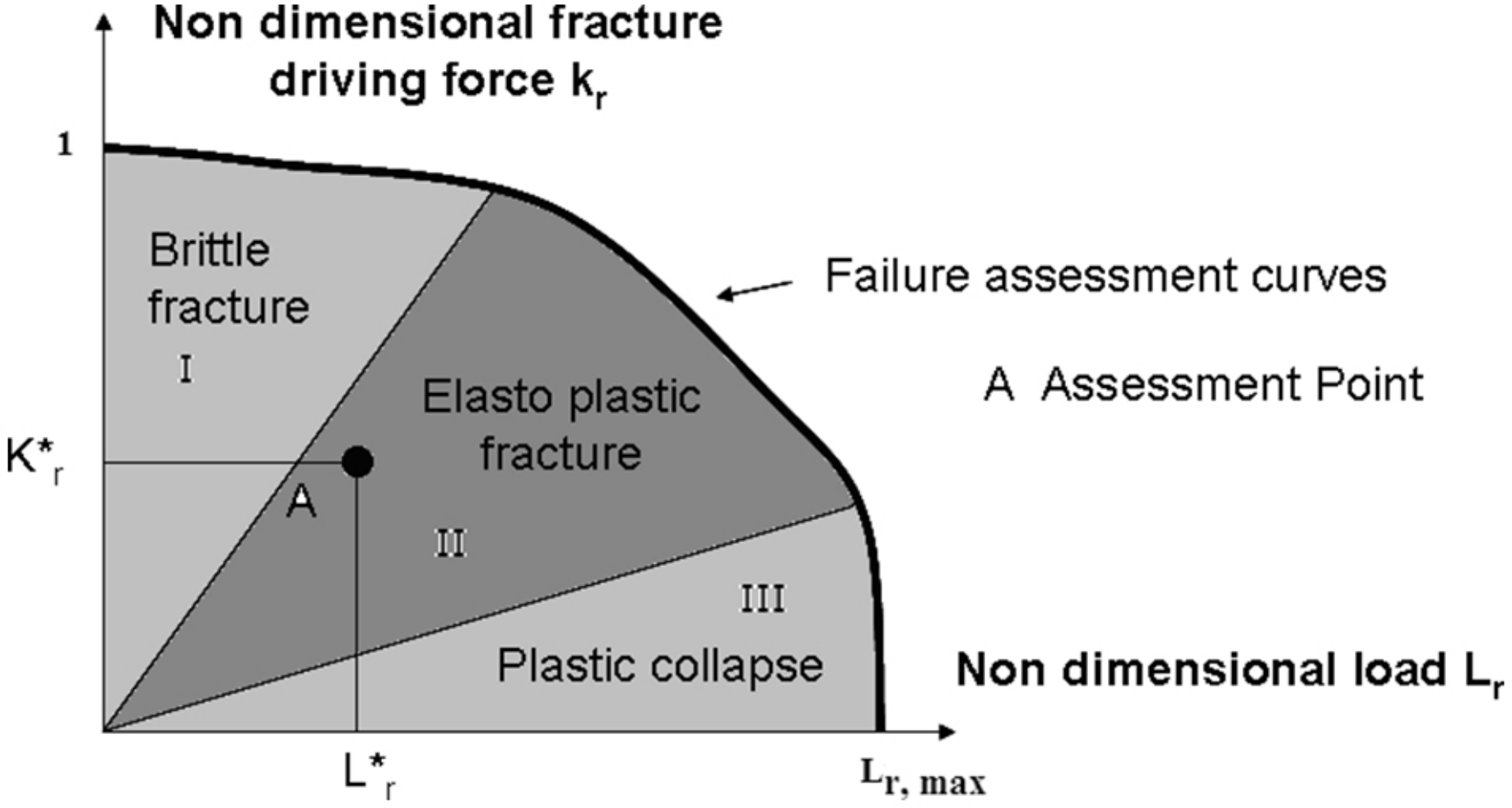
Non dimensional fracture driving force k_r
1
Brittle fracture
I
Elasto plastic fracture
II
III
Plastic collapse
Failure assessment curves
A Assessment Point
A
K^*_r
L^*_r
$L_{r,\,max}$
Non dimensional load L_r

Figure 19

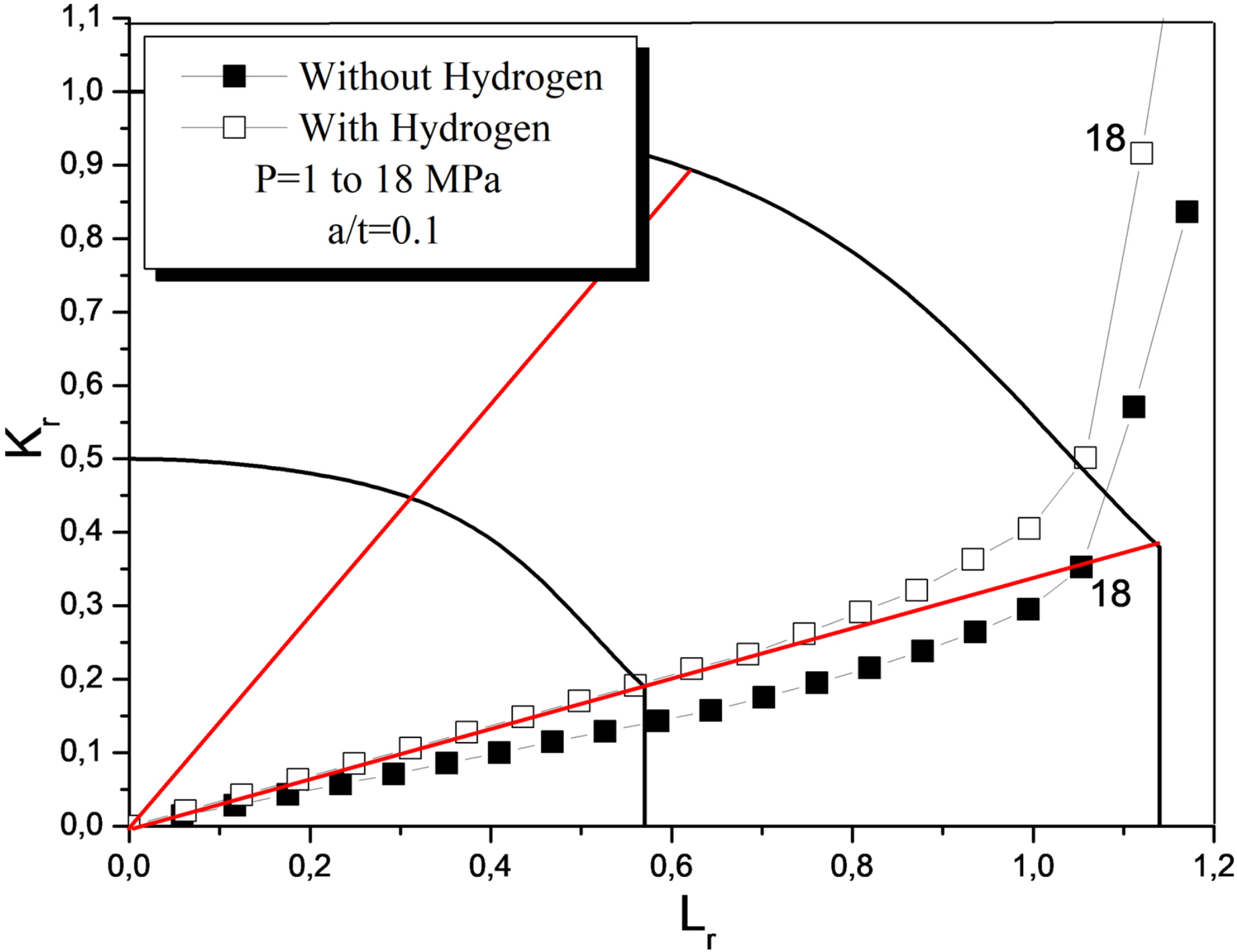
Without Hydrogen
With Hydrogen
P=1 to 18 MPa
a/t=0.1
18
18
K_r
L_r
0,0
0,1
0,2
0,3
0,4
0,5
0,6
0,7
0,8
0,9
1,0
1,1
0,0
0,2
0,4
0,6
0,8
1,0
1,2

Figure 20